arXiv:1001.1358v3 [hep-th] 27 Jan 2010

Higgs-regularized three-loop four-gluon amplitude in $\mathcal{N} = 4$ SYM: exponentiation and Regge limits

Johannes M. Henn[a], Stephen G. Naculich[1,b], Howard J. Schnitzer[2,c] and Marcus Spradlin[3,d]

[a]*Institut für Physik*
Humboldt-Universität zu Berlin, Newtonstraße15, D-12489 Berlin, Germany

[b]*Department of Physics*
Bowdoin College, Brunswick, ME 04011, USA

[c]*Theoretical Physics Group*
Martin Fisher School of Physics
Brandeis University, Waltham, MA 02454, USA

[d]*Brown University, Providence, Rhode Island 02912, USA*

Abstract

We compute the three-loop contribution to the $\mathcal{N} = 4$ supersymmetric Yang-Mills planar four-gluon amplitude using the recently-proposed Higgs IR regulator of Alday, Henn, Plefka, and Schuster. In particular, we test the proposed exponential ansatz for the four-gluon amplitude that is the analog of the BDS ansatz in dimensional regularization. By evaluating our results at a number of kinematic points, and also in several kinematic limits, we establish the validity of this ansatz at the three-loop level.

We also examine the Regge limit of the planar four-gluon amplitude using several different IR regulators: dimensional regularization, Higgs regularization, and a cutoff regularization. In the latter two schemes, it is shown that the leading logarithmic (LL) behavior of the amplitudes, and therefore the lowest-order approximation to the gluon Regge trajectory, can be correctly obtained from the ladder approximation of the sum of diagrams. In dimensional regularization, on the other hand, there is no single dominant set of diagrams in the LL approximation. We also compute the NLL and NNLL behavior of the L-loop ladder diagram using Higgs regularization.

---

1 Introduction

Recent years have witnessed significant advances in $\mathcal{N} = 4$ supersymmetric Yang-Mills theory (SYM) in four dimensions. The AdS/CFT conjecture relating $\mathcal{N} = 4$ SYM theory to maximally supersymmetric string theory on $\text{AdS}_5 \times \text{S}^5$ reveals various integrable structures. One aspect of recent progress is a greater understanding of the structure of on-shell scattering amplitudes, at both tree level and loop level. For example, based on an iterative structure found at two loops [1], Bern, Dixon and Smirnov (BDS) conjectured an all-loop form of the maximally-helicity-violating planar n-gluon amplitude [2], which is believed to be correct for $n = 4$ and 5, but requires modification by a function of cross-ratios for six or more gluons [3–7].

The simplicity of the BDS form for four- and five-gluon loop amplitudes arises from a hidden symmetry of the planar theory, viz., dual conformal invariance [8]. Dual conformal symmetry is also present in the theory at strong coupling, and can be seen in a string theory description of the scattering amplitudes, which are identified with Wilson loop expectation values in a T-dual AdS space [9]. The dual conformal symmetry of scattering amplitudes is understood as the usual conformal symmetry of the dual Wilson loops. In fact, this scattering amplitude/Wilson loop relation extends to weak coupling as well [3, 10, 11] (for reviews see [12, 13]).

The dual conformal symmetry is anomalous at loop level due to ultraviolet divergences associated with the cusps of the Wilson loops (which correspond to infrared (IR) divergences of the scattering amplitudes). Anomalous Ward identities can be derived for the Wilson loop expectation values [14], whose solution is unique up to a function of conformal cross-ratios. The BDS ansatz satisfies the anomalous Ward identity, therefore it is exact for Wilson loops with four and five cusps, since there are no cross-ratios in these cases. Assuming the Wilson loop/scattering amplitude duality, this implies the validity of the BDS ansatz for four- and five-gluon amplitudes.

Dual conformal symmetry extends to a dual superconformal symmetry [15], which is a symmetry of all tree-level amplitudes [15–17]. (This dual superconformal symmetry can also be understood from the string theory point of view by means of fermionic T-duality [18–20].) The dual superconformal symmetry combines with the conventional superconformal symmetry of $\mathcal{N} = 4$ SYM theory to form a Yangian symmetry [21]. The IR divergences of the loop amplitudes, however, *a priori* destroy both the ordinary and dual superconformal symmetries (and therefore the Yangian symmetry); this breakdown is explicitly seen in dimensional regularization. Unlike the dual conformal symmetry, the breaking of the ordinary conformal symmetry is not (yet) under control (see however refs. [22–24] for progress in this direction), and so the role of the Yangian symmetry for loop amplitudes is unclear.

In practice, it is desirable to use a regulator that preserves as many symmetries as possible. Recently, Alday, Henn, Plefka, and Schuster (AHPS) presented a regulator which, in contrast to dimensional regularization, leaves the dual conformal symmetry unbroken [25]. In this approach, the SYM theory is considered on the Coulomb branch where scalar vevs break the gauge symmetry, causing some of the gauge bosons to become massive through the Higgs mechanism. Planar gluon scattering amplitudes on this branch can be computed using scalar diagrams in which some of the internal and external states are massive, regulating the IR divergences of the scattering amplitudes (for earlier references see [9, 26–28]). The diagrams remain dual conformal invariant,

however, provided that the dual conformal generators are taken to act on the masses as well as on the kinematical variables. The diagrams that can appear in the scattering amplitudes are highly constrained by the assumption of (extended) dual conformal symmetry. There is one point in moduli space for which all the lines along the periphery of the diagrams have mass m, while the external states and the lines in the interior of the diagram are all massless. This is believed to be sufficient to regulate all IR divergences of planar scattering amplitudes. The original SYM theory is then recovered by taking m small.

Using this Higgs regulator, AHPS computed the $\mathcal{N} = 4$ SYM four-gluon amplitude at one and two loops. They showed that the planar two-loop amplitude satisfies an iterative relation analogous to the one that holds in dimensional regularization [1], and suggested that exponentiation might extend to higher loops in an analog of the BDS ansatz for the four-gluon amplitude:

$$
\begin{aligned}
\log M(s,t) &= -\frac{1}{8}\gamma(a)\left[\log^2\left(\frac{s}{m^2}\right) + \log^2\left(\frac{t}{m^2}\right)\right] - \tilde{\mathcal{G}}_0(a)\left[\log\left(\frac{s}{m^2}\right) + \log\left(\frac{t}{m^2}\right)\right] \\
&\quad + \frac{1}{8}\gamma(a)\left[\log^2\left(\frac{s}{t}\right) + \pi^2\right] + \tilde{c}(a) + \mathcal{O}(m^2)
\end{aligned}
\tag{1.1}
$$

where $M(s,t)$ is the ratio of the all-orders planar amplitude to the tree-level amplitude, $\gamma(a)$ is the cusp anomalous dimension (3.3), and $\tilde{\mathcal{G}}_0(a)$ and $\tilde{c}(a)$ are analogs of functions appearing in the BDS ansatz in dimensional regularization (3.5). Let us emphasize that the nontrivial content of the BDS ansatz is the statement about the finite terms; the IR singular terms of the amplitude are expected to obey eq. (1.1) (or eq. (3.5)) on general field theory grounds.[4]

In this paper, we explore whether eq. (1.1) continues to hold at three loops and beyond. We compute the three-loop four-gluon amplitude using Higgs regularization, assuming that only integrals invariant under (extended) dual conformal symmetry contribute. Mellin-Barnes techniques are used to evaluate the integrals, some parts of which are computed numerically. We numerically evaluate the results at a number of kinematic points, and obtain explicit expressions in several kinematic limits (e.g., $s = t$ and also the Regge limit $s \gg t$). In every case, our results confirm the expected exponential ansatz (1.1) at the three-loop level.

An important difference between Higgs regularization and dimensional regularization is that in the former, IR divergences take the form of logarithms of m^2 whereas in the latter, IR divergences appear as poles in ϵ, where $D = 4 - 2\epsilon$. A consequence of this is that, provided eq. (1.1) is valid, the L-loop amplitude in Higgs regularization may be computed by simply exponentiating $\log M(s,t)$ without regard for the $\mathcal{O}(m^2)$ terms since they continue to vanish as $m \to 0$ even when multiplied by logarithms of m^2. In contrast, the BDS ansatz in dimensional regularization (3.5) specifies $\log M(s,t)$ up to terms that vanish as $\epsilon \to 0$. In exponentiating $\log M(s,t)$, these neglected terms can combine with the IR poles to give rather complicated contributions to the IR-finite L-loop amplitude.

---

[4]In ref. [29] the transition from amplitudes in dimensional regularization to amplitudes where (part of) the IR divergences are regulated by (small) masses was investigated. In this way, the $\log^2(m^2)$ and $\log(m^2)$ terms in eq. (1.1) can be understood as arising from a different multiplicative renormalization factor relative to dimensional regularization. It is also conceivable that by adapting the formalism of ref. [29] to the present case one could show that the terms finite as $m^2 \to 0$ follow from the corresponding formula in dimensional regularization. This would imply that the BDS ansatz can be stated in a scheme-independent way.

To put the matter the other way around, in order to test eq. (1.1) one need not compute any $\mathcal{O}(m^2)$ terms of the Higgs-regulated L-loop amplitudes because they cannot make any contribution to the IR-finite part of $\log M(s,t)$, whereas to test the BDS ansatz in dimensional regularization, one must compute $\mathcal{O}(\epsilon)$ and higher terms in the lower-loop amplitudes to obtain all the IR-finite contributions to $\log M(s,t)$. This is one of several significant advantages that Higgs-regulated amplitudes have over their dimensionally-regulated counterparts.

A second major focus of this paper is the Regge behavior of planar $\mathcal{N} = 4$ SYM amplitudes using Higgs regularization. One motivation for this is that it presents a different way of examining the iterative structure of the theory, in which some results can be obtained to all orders. Equation (1.1) may be rewritten as

$$\log M(s,t) = \left[-\frac{1}{4}\gamma(a)\log\left(\frac{t}{m^2}\right) - \tilde{\mathcal{G}}_0(a) \right] \log\left(\frac{s}{m^2}\right) - \tilde{\mathcal{G}}_0(a)\log\left(\frac{t}{m^2}\right) + \frac{\pi^2}{8}\gamma(a) + \tilde{c}(a) + \mathcal{O}(m^2)$$

(1.2)

in which the $\log^2(s/m^2)$ terms have cancelled[5] to leave a single $\log(s/m^2)$. Consequently, $M(s,t)$ exhibits exact Regge behavior

$$M(s,t) = M(t,s) = \beta(t)\left(\frac{s}{m^2}\right)^{\alpha(t)-1}$$

(1.3)

where the all-loop-orders Regge trajectory is

$$\alpha(t) - 1 = -\frac{1}{4}\gamma(a)\log\left(\frac{t}{m^2}\right) - \tilde{\mathcal{G}}_0(a).$$

(1.4)

The lowest order term of the trajectory, $-a\log(t/m^2)$, gives rise to the leading log (LL) behavior of the L-loop amplitude

$$M^{(L)}(s,t) \quad \underset{s \gg t}{\longrightarrow} \quad \frac{(-1)^L}{L!}\log^L\left(\frac{t}{m^2}\right)\log^L\left(\frac{s}{m^2}\right)$$

(1.5)

in the Regge limit, whereas higher-order terms in the cusp anomalous dimension contribute to the NLL (next-to-leading-log), NNLL, etc. pieces of the amplitude (see eq. (4.10)).

There is a subtle question of order of limits that appears when considering the Regge limit. In fact there are two ways this limit can be taken. The first possibility (a) consists in taking the limit $m^2 \ll s, t$ first, and then taking the limit $s \gg t$. This order is implicit in eq. (1.2). The second possibility (b) consists in taking the limit $s \gg t, m^2$ first, and then taking $m^2 \ll t$. A priori, it is not clear that the result will not depend on the way the limit is taken. Explicit calculation shows that no such ambiguity arises for the integrals appearing at one and two loops. At three loops, as we will show, the individual integrals give different contributions in the two limits; the three-loop amplitude $M^{(3)}(s,t)$, however, is unchanged.

It seems that both ways of taking the limit can be justified, with slightly different interpretations.[6] On the one hand, the Regge (a) limit seems more appropriate in order to make

---

[5]A similar cancellation occurs in the Regge limit using dimensional regularization [10,30–32]. Subleading-color corrections to the Regge trajectory in dimensional regularization were also considered in ref. [32].

[6]There is an analogous question in dimensional regularization of whether to take $\epsilon \to 0$ or $s \gg t$ first [33], but see the Erratum in **v5** [34].

contact with results in the massless theory. On the other hand, the Regge (b) limit is natural for scattering amplitudes with masses (see ref. [35] and sec. 4.4 below).

We show in this paper that the leading log behavior (1.5) stems entirely from a single scalar diagram, the vertical ladder, in the Regge (b) limit of the Higgs-regularized loop expansion. (This contrasts with dimensional regularization, in which ladder diagrams do not dominate in the Regge limit; the leading log behavior of the L-loop amplitude receives contributions from most of the contributing diagrams. This might have significant implications for recent discussions of multi-Regge behavior [33, 36–40].) We also compute the NLL and NNLL terms of the L-loop vertical ladder diagram. Other Higgs-regularized diagrams also contribute to the NLL, NNLL, etc. terms of the amplitude, although we do not yet have an all-orders characterization of which diagrams contribute to each order in the leading log expansion.

In ref. [41], the LL approximation to the gluon Regge trajectory was computed using a ladder approximation and an alternative IR regulator, in which the external lines are massless while all internal lines of the diagrams are given a common mass (which cuts off the IR divergences)[7]. In the LL limit, this "cutoff regulator" yields results identical to those found in this paper.[8] The reason for this, as we will see, is that the LL approximation to the vertical ladder is insensitive to the masses of the propagators constituting the rungs of the ladder, and this is the only difference between the cutoff and Higgs regulators. We also compute the NLL contribution to the L-loop vertical ladder diagram using the cutoff regulator, which differs from the Higgs regulator by scheme-dependent constants.

The Regge (b) limit of the scattering amplitudes can be understood by performing the Higgs regularization at a different point on the Coulomb branch of the theory. In this case, the scattered particles are massive, whereas some of the internal lines remain massless, eliminating the collinear but not the soft IR divergences. We suggest how the Regge behavior of the four-point amplitude can be understood from the cusp anomalous dimension of a Wilson line with a non-light-like cusp.

The paper is organized as follows: In sec. 2, we give a short review of dual conformal symmetry. Exponentiation of the planar four-gluon amplitude in dimensional regularization and in Higgs regularization are discussed in section 3, and the three-loop amplitude in Higgs regularization is computed. The Regge limit of the planar four-gluon amplitude in several regularization schemes is examined in sec. 4, and the first three terms in the leading log expansion of the L-loop vertical ladder diagram are computed. Most of the technical details are relegated to three appendices.

2   Short review of dual conformal symmetry

In this section we give a short review of dual conformal symmetry, with a particular focus on four-gluon amplitudes. Hints for dual conformal symmetry first appeared as an observation that

---

[7]This procedure is closely related to an off-shell regulator. If all physical states have a common mass m arising from a conventional Higgs mechanism, then external lines with $p^2 = 0$ are off-shell from this point of view.

[8]The Higgs regulator considered in this paper does not seem directly applicable to computing the subleading-color contributions of $\mathcal{N} = 4$ SYM amplitudes, which are not dual-conformal-invariant, and which involve non-planar diagrams. The cutoff regulator might be more suitable in this respect.

the loop integrals contributing to planar four-gluon scattering amplitudes in $\mathcal{N} = 4$ SYM theory have special properties when written in a dual coordinate space [8].

Let us recall that the full four-gluon amplitude can be decomposed in a trace basis, the coefficients of which are referred to as color-ordered amplitudes [42–44]. The color-ordered planar (i.e., large N) amplitudes may be written in a loop expansion

$$A(p_i, \varepsilon_i) = \sum_{L=0}^{\infty} a^L A^{(L)}(p_i, \varepsilon_i) \tag{2.1}$$

in the 't Hooft parameter [2]

$$a \equiv \frac{g^2 N}{8\pi^2} \left(4\pi \, \mathrm{e}^{-\gamma_{\mathrm{E}}}\right)^{\epsilon} \tag{2.2}$$

where γ_{E} is Euler's constant, and $\epsilon = \frac{1}{2}(4 - D)$ with $\epsilon < 0$ to regulate IR divergences. In $\mathcal{N} = 4$ SYM theory, loop corrections to the four-gluon amplitude have the same helicity dependence as the tree amplitude, so we factor out the tree amplitude to express the amplitude as a function $M(s, t)$ of the kinematic variables $s = (p_1 + p_2)^2$ and $t = (p_2 + p_3)^2$ only[9]

$$A(p_i, \varepsilon_i) \equiv A^{(0)}(p_i, \varepsilon_i) \, M(s, t), \qquad M(s, t) = 1 + \sum_{L=1}^{\infty} a^L M^{(L)}(s, t) \,. \tag{2.3}$$

At one loop, we have

$$M^{(1)}(s, t) = -\frac{1}{2} I_1(s, t) \tag{2.4}$$

with the one-loop integral I_1 given by

$$I_1(s, t) = \left(e^{\gamma_{\mathrm{E}}} \mu^2\right)^{\epsilon} \int \frac{d^D k}{i\pi^{D/2}} \frac{(p_1 + p_2)^2 (p_2 + p_3)^2}{k^2 (k + p_1)^2 (k + p_1 + p_2)^2 (k - p_4)^2} \,, \tag{2.5}$$

where the external states are on-shell: $p_i^2 = 0$. After a change of variables to a dual coordinate space [8, 45],

$$p_i^{\mu} = x_i^{\mu} - x_{i+1}^{\mu}, \qquad x_5 \equiv x_1 \,, \tag{2.6}$$

one obtains

$$I_1(s, t) = \left(e^{\gamma_{\mathrm{E}}} \mu^2\right)^{\epsilon} \int \frac{d^D x_a}{i\pi^{D/2}} \frac{x_{13}^2 x_{24}^2}{x_{1a}^2 x_{2a}^2 x_{3a}^2 x_{4a}^2} \,, \tag{2.7}$$

where now the on-shell conditions read $x_{i,i+1}^2 = 0$. Note that this change of variables can be most easily done in a graphical way (see fig. 1). From eq. (2.7) one can see that for $D = 4$ the integral would be invariant under conformal transformations in the dual coordinate space [8, 45]; hence the name "dual conformal symmetry." Due to infrared divergences one cannot set $D = 4$, and hence the aforementioned symmetry is broken, which is why such integrals were later called "pseudoconformal." It was found that at least up to four loops all integrals appearing in the

---

[9]In this paper, we follow the $- + + +$ metric conventions of ref. [25], so that s is negative for positive CM energy. The amplitude $M(s, t)$ will be real for s and t both positive.
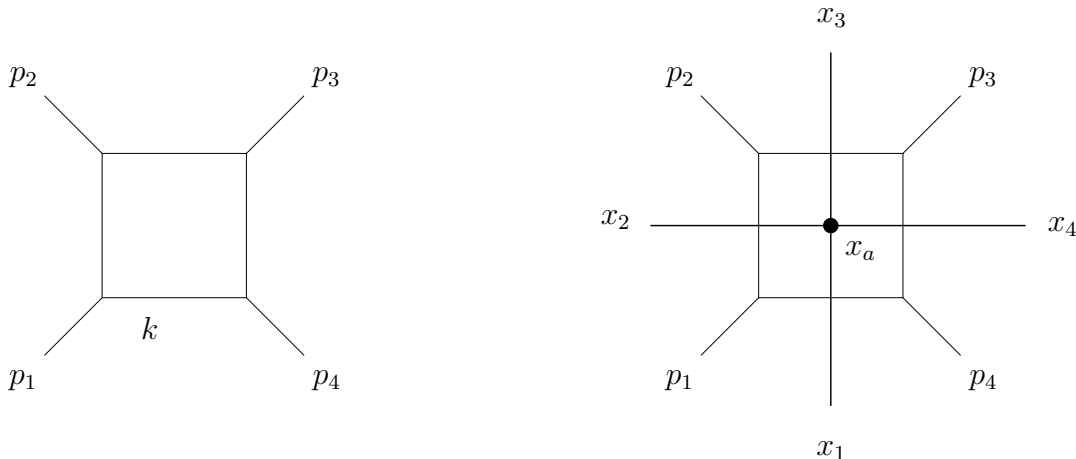
Figure 1: One-loop scalar box diagram representing the on-shell integral (2.5) together with its dual diagram (2.7). The numerator factor $(p_1 + p_2)^2(p_2 + p_3)^2 = x_{13}^2 x_{24}^2$ is not displayed.

four-particle scattering amplitude have this property [10, 46]. All this hinted at some deeper underlying structure.

From the practical point of view, assuming that only pseudoconformal integrals contribute to an amplitude proved to be a useful guiding principle[10] (see e.g. refs. [5, 47]). On the other hand, the inevitable breaking of the symmetry for $D \neq 4$ was not under control. This changed when it was realized that the (finite part of the) logarithm of the amplitude satisfies certain anomalous Ward identities, which were initially derived for Wilson loops and are conjectured to hold for scattering amplitudes as well. Assuming the Ward identities hold for the scattering amplitudes, they explain the correctness of the BDS ansatz for four and five scattered particles [3, 14].

Initially dual conformal symmetry could be applied to the n-gluon amplitude M_n for maximally-helicity-violating (MHV) amplitudes only, as can be seen from the fact that the variables in eq. (2.6) do not carry helicity. In ref. [15], it was shown how to incorporate the helicity information and to define dual (super)conformal symmetry for arbitrary amplitudes, both MHV and non-MHV. The predictions of ref. [15] about how dual conformal symmetry is realized at tree and loop level (through an anomalous Ward identity) have by now been checked to one-loop order [48–51]. The status of dual *super*conformal symmetry at loop level, which is related to the conventional superconformal symmetry, is under investigation [22–24].

The symmetries mentioned above can also be seen at strong coupling using the AdS/CFT correspondence. In a groundbreaking paper [9], a prescription for computing scattering amplitudes at strong coupling was given. There, a bosonic T-duality was used that maps the original AdS space to a dual AdS space. Dual conformal symmetry can then be identified with the isometries of the dual AdS space (up to the issue of regularization). It was later shown that the bosonic T-duality can be supplemented with a fermionic T-duality [18–20], which leads to the counterpart of the dual superconformal symmetry found in the field theory. The analysis of

---

[10]Note that there can be subtleties about which integrals should be called pseudoconformal (see e.g. ref. [5]), having to do with the peculiarities of dimensional regularization/reduction.

ref. [18] is valid to all orders in the gauge coupling constant; however, just as in the field theory, introducing a regulator may break the symmetry. It would be interesting to address this question in the string theory approach. A somewhat related question is how the helicity dependence of the scattering amplitudes is encoded in the string theory setup. (At strong coupling, it is argued to be an overall factor, which can be ignored, but certainly this is not the case at lower orders in the coupling constant.)

In a recent paper [25], a new regularization of planar amplitudes inspired by the string theory setup of refs. [9, 18] was advocated (see also refs. [26–28]). In the string theory, besides the usual stack of N branes at $z = 0$ (z being the radial AdS coordinate, with the AdS radius normalized to unity), M further branes are placed at distances $z_i = 1/m_i$. The scattering takes place on the stack of M branes. In the field theory, this corresponds to going to the Coulomb branch of $\mathcal{N} = 4$ SYM. Specifically, one starts with a gauge group $U(N + M)$ and breaks it to $U(N) \times U(M) \to U(N) \times U(1)^M$. This leads to masses $|m_{i_1} - m_{i_2}|$ for fields with labels in the $U(M)$, masses $|m_i|$ for fields with mixed N, M gauge labels, while the $U(N)$ fields remain massless. We then consider the scattering of fields with indices in the $U(M)$ part of the gauge group and take $N \gg M$. (In other words, we drop all diagrams containing loops of particles with gauge indices M.) Therefore, the internal labels will all be in the N part of the gauge group, while the particles running along the perimeter of all Feynman diagrams will have mixed (M, N) labels, and hence will have massive propagators. The latter make the integrals IR finite, and there is no need to use dimensional regularization. Of course, strictly speaking one is considering a different theory, but the original theory is approached in the small mass limit.[11]

The string theory setup suggests that the planar amplitudes defined in this way should have an exact, i.e. unbroken, dual conformal symmetry. This is possible because there are now additional terms in the dual conformal generators that act on the Higgs masses. These additional terms come from the isometries of dual AdS space. At one loop, the integral (2.7) is replaced by

$$I_1(s, t; m_1, m_2, m_3, m_4) = \int \frac{d^4 x_a}{i\pi^2} \frac{(x_{13}^2 + (m_1 - m_3)^2)(x_{24}^2 + (m_2 - m_4)^2)}{(x_{1a}^2 + m_1^2)(x_{2a}^2 + m_2^2)(x_{3a}^2 + m_3^2)(x_{4a}^2 + m_4^2)}, \qquad (2.8)$$

now subject to the on-shell conditions $x_{i,i+1}^2 = -(m_i - m_{i+1})^2$, with the identification $m_5 \equiv m_1$. As anticipated, I_1 is annihilated by the extended form of dual conformal transformations,[12]

$$\hat{K}^\mu I_1 = 0, \qquad (2.9)$$

where

$$\hat{K}_\mu = \sum_{i=1}^4 \left[2x_{i\mu} \left(x_i^\nu \frac{\partial}{\partial x_i^\nu} + m_i \frac{\partial}{\partial m_i} \right) - (x_i^2 + m_i^2) \frac{\partial}{\partial x_i^\mu} \right]. \qquad (2.10)$$

---

[11]Unfortunately, since the requirement of finiteness imposes keeping $N \gg M$, one cannot reproduce the non-planar scattering amplitudes of the original theory.

[12]This can be seen most easily by thinking of the masses m_i as a fifth coordinate of the dual coordinates, defining $\hat{x}_i^M \equiv (x_i^\mu, m_i)$, and considering conformal inversions in this five-dimensional space. For further details, see ref. [25].
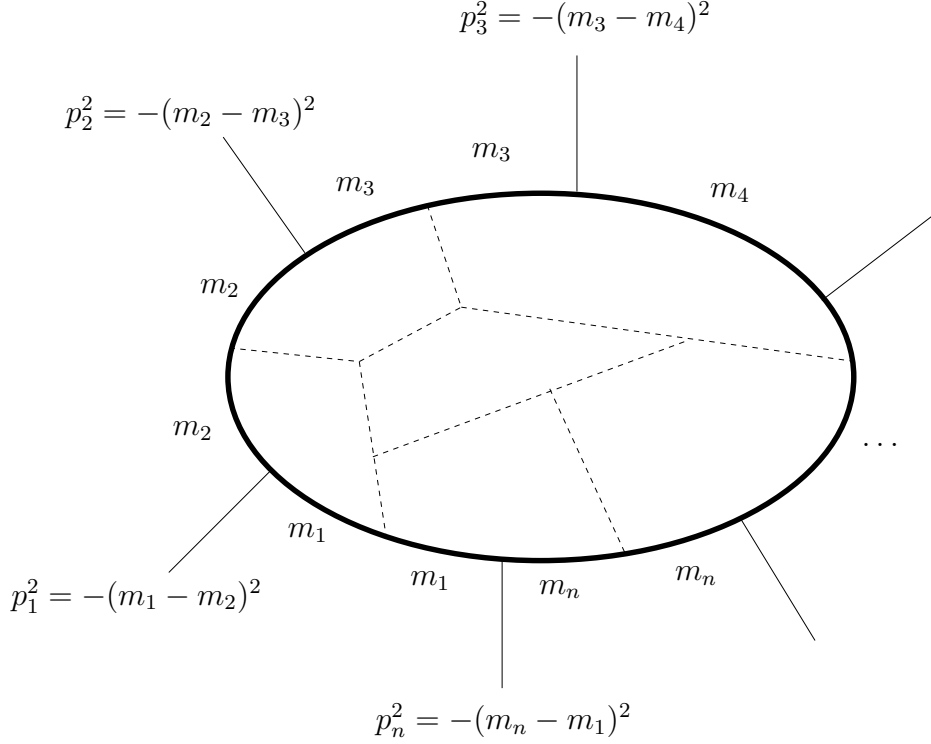
Figure 2: Mass assignment of a generic planar diagram in the Higgs setup. The external lines correspond to on-shell particles with $p_i^2 = -(m_i - m_{i+1})^2$. The internal dashed lines correspond to massless particles. We call particles of mass $|m_i - m_{i+1}|$ 'light' and particles of mass m_i 'heavy' since the former become massless when we consider the equal mass case $m_i = m$.

Note that the integral is finite (for $m_i \neq 0$), and the symmetry is exact (i.e. unbroken), hence there is no anomaly term on the r.h.s. of eq. (2.9). From eq. (2.9) one can deduce that the functional dependence of I_1 is [25]

$$I_1(s, t; m_1, m_2, m_3, m_4) = f(u, v), \tag{2.11}$$

where

$$u = \frac{m_1 m_3}{s + (m_1 - m_3)^2} \qquad \text{and} \qquad v = \frac{m_2 m_4}{t + (m_2 - m_4)^2}. \tag{2.12}$$

Similar restrictions hold for a higher number of external legs. This form of dual conformal invariance in the field theory was checked for a particular four-scalar amplitude at one loop [25]. There it was also shown that assuming this symmetry at two loops leads to an iterative relation similar to that which holds in dimensional regularization.

In fig. 2, we illustrate where the Higgs masses appear in a generic n-point integral in this setup. Thanks to dual conformal symmetry, we can set all masses equal without loss of generality, in which case all external particles are massless, the particles in the outer loop of a diagram are massive, and all particles on the inside are massless.

One can in principle write down all dual conformal integrals at a given loop order and for a given number n of external legs. The amplitude would then be given by a linear combination of

these integrals [10]

$$M_n = 1 + \sum_{\mathcal{I}} a^{L(\mathcal{I})} c(\mathcal{I}) \, \mathcal{I} \, , \tag{2.13}$$

where the sum runs over all dual conformal integrals[13] $\mathcal{I}$, with $L(\mathcal{I})$ the loop order of the integral, and $c(\mathcal{I})$ a (rational) coefficient (a number in the case of MHV amplitudes). Further restrictions result from the requirement that the diagrams must arise from a scattering process; for example, at two loops, the one-loop integral (2.8) cannot appear squared. Moreover, there are restrictions on the number of propagators and numerator factors. Finally, integrals that would be formally dual conformal invariant but are divergent despite the introduction of the Higgs regulator should not appear [10].

3 Exponentiation of the four-gluon amplitude

In this section, we recall the exponentiation of the four-point amplitude of $\mathcal{N} = 4$ SYM theory, first using dimensional regularization to regulate the IR divergences, and then using the Higgs regularization described in sec. 2.

3.1 Exponentiation in dimensional regularization

On the basis of ref. [1], Bern, Dixon, and Smirnov conjectured [2] that the dimensionally-regularized all-loop orders amplitude (2.3) satisfies

$$\log M(s,t) = \sum_{\ell=1}^{\infty} a^{\ell} \left[f^{(\ell)}(\epsilon) M^{(1)}(s,t;\ell\epsilon) + C^{(\ell)} + \mathcal{O}(\epsilon) \right] \tag{3.1}$$

where $M^{(1)}(s,t)$ is given by eq. (2.4), $\epsilon = \frac{1}{2}(4 - D)$, and

$$f^{(\ell)}(\epsilon) = \frac{1}{4}\gamma^{(\ell)} + \frac{1}{2}\epsilon\,\ell\,\mathcal{G}_0^{(\ell)} + \epsilon^2 f_2^{(\ell)} \tag{3.2}$$

with the cusp $\gamma^{(\ell)}$ and collinear $\mathcal{G}_0^{(\ell)}$ anomalous dimensions [52] given by[14]

$$\gamma(a) = \sum_{\ell=1}^{\infty} a^{\ell} \gamma^{(\ell)} = 4a - 4\zeta_2 a^2 + 22\zeta_4 a^3 + \cdots \tag{3.3}$$

$$\mathcal{G}_0(a) = \sum_{\ell=1}^{\infty} a^{\ell} \mathcal{G}_0^{(\ell)} = -\zeta_3 a^2 + \left(4\zeta_5 + \frac{10}{3}\zeta_2\zeta_3 \right) a^3 + \cdots \tag{3.4}$$

---

[13]Here we mean dual conformal integrals in the sense of the Higgs regulator of ref. [25], not the off-shell regulator of ref. [10].

[14]We use the notation of ref. [2]. Note that $\gamma(a) = 2\,\Gamma_{\text{cusp}}(a)$, where $\Gamma_{\text{cusp}}(a)$ is also widely used in the literature.

The constants $C^{(\ell)}$ and $f_2^{(\ell)}$ and the $\mathcal{O}(\epsilon)$ terms in eq. (3.1) are not known *a priori*. The BDS ansatz (3.1) may be re-expressed as

$$\log M(s,t) = \sum_{\ell=1}^{\infty} a^\ell \left[-\frac{\gamma^{(\ell)}}{4(\ell\epsilon)^2} - \frac{\mathcal{G}_0^{(\ell)}}{2\ell\epsilon} \right] \left[\left(\frac{\mu^2}{s}\right)^{\ell\epsilon} + \left(\frac{\mu^2}{t}\right)^{\ell\epsilon} \right] + \frac{\gamma(a)}{8}\left[\log^2\left(\frac{s}{t}\right) + \frac{4}{3}\pi^2\right] + c(a) + \mathcal{O}(\epsilon) \tag{3.5}$$

where [2]

$$c(a) = \sum_{\ell=1}^{\infty} a^\ell c^{(\ell)} = \sum_{\ell=1}^{\infty} a^\ell \left[-\frac{2f_2^{(\ell)}}{\ell^2} + C^{(\ell)} \right] = -\frac{\pi^4}{120}a^2 + \left(\frac{341}{216}\zeta_6 - \frac{17}{9}\zeta_3^2\right)a^3 + \cdots \tag{3.6}$$

Overlapping soft and collinear IR divergences are responsible for the $1/\epsilon^2$ pole in eq. (3.5).

While the BDS ansatz (3.5) implies that the IR-finite part of the *logarithm* of the amplitude is simply expressible in terms of $\log(s/\mu^2)$ and $\log(t/\mu^2)$ and a set of constants $\gamma^{(\ell)}$, $\mathcal{G}_0^{(\ell)}$, and $c^{(\ell)}$, the same is not true of the L-loop amplitudes $M^{(L)}(s,t)$ themselves. For example, eq. (3.5) implies [1]

$$\begin{aligned}
M^{(2)}(s,t) &= \frac{1}{2}\left[M^{(1)}(s,t)\right]^2 - \frac{\gamma^{(2)}}{8\epsilon^2} - \frac{\mathcal{G}_0^{(2)}}{2\epsilon} + \frac{\gamma^{(2)}}{8\epsilon}\left[\log\left(\frac{s}{\mu^2}\right) + \log\left(\frac{t}{\mu^2}\right)\right] \\
&+ \frac{\mathcal{G}_0^{(2)}}{2}\left[\log\left(\frac{s}{\mu^2}\right) + \log\left(\frac{t}{\mu^2}\right)\right] - \frac{\gamma^{(2)}}{4}\log\left(\frac{s}{\mu^2}\right)\log\left(\frac{t}{\mu^2}\right) + \frac{\pi^2}{6}\gamma^{(2)} + c^{(2)} + \mathcal{O}(\epsilon).
\end{aligned} \tag{3.7}$$

Because of interference between the positive and negative powers of ϵ in $\left[M^{(1)}(s,t)\right]^2$, the $\mathcal{O}(\epsilon^{-1})$ and $\mathcal{O}(\epsilon^0)$ terms [53] in $M^{(2)}(s,t)$ depend on more complicated functions (polylogarithms) of s and t, which are present in the $\mathcal{O}(\epsilon)$ and $\mathcal{O}(\epsilon^2)$ terms [1] of $M^{(1)}(s,t)$. In general $M^{(L)}(s,t)$ will receive contributions from the coefficients of positive powers of ϵ in all lower-loop amplitudes.

3.2 Exponentiation in Higgs regularization

The Higgs mechanism reviewed in section 2 can be used as a gauge-invariant regulator of the IR divergences in the planar massless theory, with the IR divergences appearing as $\log(m^2)$ terms in the amplitude, and any terms that vanish as $m \to 0$ are dropped. One could ask whether, when regulated in this way, the four-point loop amplitude satisfies iterative relations similar to the BDS ansatz for the dimensionally-regulated amplitude. In ref. [25], it was suggested that the analog of eq. (3.5) is

$$\begin{aligned}
\log M(s,t) &= -\frac{1}{8}\gamma(a)\left[\log^2\left(\frac{s}{m^2}\right) + \log^2\left(\frac{t}{m^2}\right)\right] - \tilde{\mathcal{G}}_0(a)\left[\log\left(\frac{s}{m^2}\right) + \log\left(\frac{t}{m^2}\right)\right] \\
&+ \frac{1}{8}\gamma(a)\left[\log^2\left(\frac{s}{t}\right) + \pi^2\right] + \tilde{c}(a) + \mathcal{O}(m^2)
\end{aligned} \tag{3.8}$$

where $\gamma(a)$ is the cusp anomalous dimension (3.3), and $\tilde{\mathcal{G}}_0(a)$ and $\tilde{c}(a)$ are the analogs of $\mathcal{G}_0(a)$ and $c(a)$, but need not be the same functions since they are scheme-dependent [25]. Overlapping soft and collinear IR divergences[15] are responsible for the double logarithms in eq. (3.8).

The L-loop amplitudes $M^{(L)}(s,t)$ are obtained by exponentiating eq. (3.8). In contrast to dimensional regularization, there is no interference between the IR-divergent $\log(m^2)$ terms and the $\mathcal{O}(m^2)$ terms in eq. (3.8) since such terms vanish for $m \to 0$ order by order in the coupling constant. Hence the amplitudes are simply expressed in terms of products of $\log(s/m^2)$ and $\log(t/m^2)$ and a set of constants $\gamma^{(\ell)}$, $\tilde{\mathcal{G}}_0^{(\ell)}$, and $\tilde{c}^{(\ell)}$. For comparison with later calculations, we explicitly write the predictions for the first few loop amplitudes, with $u \equiv m^2/s$ and $v \equiv m^2/t$,

$$M^{(1)} = -\log(v)\log(u) + \frac{1}{2}\pi^2 + \mathcal{O}(m^2), \tag{3.9}$$

$$\begin{aligned} M^{(2)} &= \frac{1}{2}\log^2(v)\log^2(u) - \left(\frac{1}{2}\pi^2 + \frac{1}{4}\gamma^{(2)}\right)\log(v)\log(u) \\ &+ \tilde{\mathcal{G}}_0^{(2)}\left[\log(u) + \log(v)\right] + \left(\frac{1}{8}\pi^4 + \frac{1}{8}\pi^2\gamma^{(2)} + \tilde{c}^{(2)}\right) + \mathcal{O}(m^2), \end{aligned} \tag{3.10}$$

$$\begin{aligned} M^{(3)} &= -\frac{1}{6}\log^3(v)\log^3(u) + \left(\frac{1}{4}\pi^2 + \frac{1}{4}\gamma^{(2)}\right)\log^2(v)\log^2(u) \\ &- \tilde{\mathcal{G}}_0^{(2)}\left[\log^2(v)\log(u) + \log(v)\log^2(u)\right] \\ &- \left(\frac{1}{8}\pi^4 + \frac{1}{4}\pi^2\gamma^{(2)} + \tilde{c}^{(2)} + \frac{1}{4}\gamma^{(3)}\right)\log(v)\log(u) \\ &+ \left(\frac{1}{2}\pi^2\tilde{\mathcal{G}}_0^{(2)} + \tilde{\mathcal{G}}_0^{(3)}\right)\left[\log(u) + \log(v)\right] \\ &+ \left(\frac{1}{48}\pi^6 + \frac{1}{16}\pi^4\gamma^{(2)} + \frac{1}{2}\pi^2\tilde{c}^{(2)} + \frac{1}{8}\pi^2\gamma^{(3)} + \tilde{c}^{(3)}\right) + \mathcal{O}(m^2), \end{aligned} \tag{3.11}$$

where we have explicitly set $\gamma^{(1)} = 4$ and $\tilde{\mathcal{G}}_0^{(1)} = \tilde{c}^{(1)} = 0$.

The dual-conformal integrals that contribute through two loops are (see figs. 1 and 3)

$$M(s,t) = 1 - \frac{a}{2}I_1(s,t,m^2) + \frac{a^2}{4}\left[I_2(s,t,m^2) + I_2(t,s,m^2)\right] + \mathcal{O}(a^3). \tag{3.12}$$

These integrals were computed in ref. [25], and the exponential ansatz (3.8) was verified to two-loop order. To determine the values of the constants in eqs. (3.9) and (3.10), it is sufficient to evaluate eq. (3.12) at $s = t$. Defining $x \equiv m^2/s = m^2/t$, one finds [25]

$$I_1(x) = 2\log^2(x) - \pi^2 + \mathcal{O}(x), \tag{3.13}$$

$$I_2(x) = \log^4(x) - \frac{2}{3}\pi^2\log^2(x) - 4\zeta_3\log(x) + \frac{1}{10}\pi^4 + \mathcal{O}(x). \tag{3.14}$$

---

[15]In sec. 4.4, we will see that only soft divergences contribute in the Regge limit, giving a single logarithmic divergence.
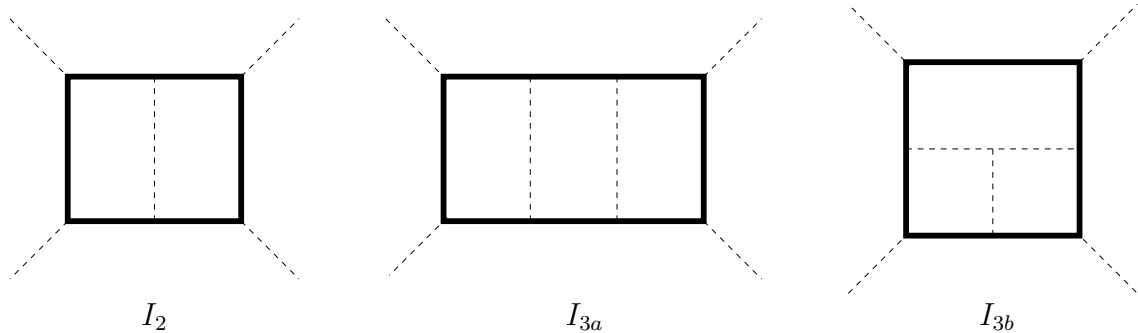
Figure 3: Two- and three-loop four-point dual conformal diagrams. I_2 and I_{3a} are ladder diagrams; I_{3b} is the tennis-court diagram. Numerator factors (including a loop-momentum-dependent factor for the tennis court) are omitted. See eqs. (A.20) and (A.23) for explicit formulae for the integrals.
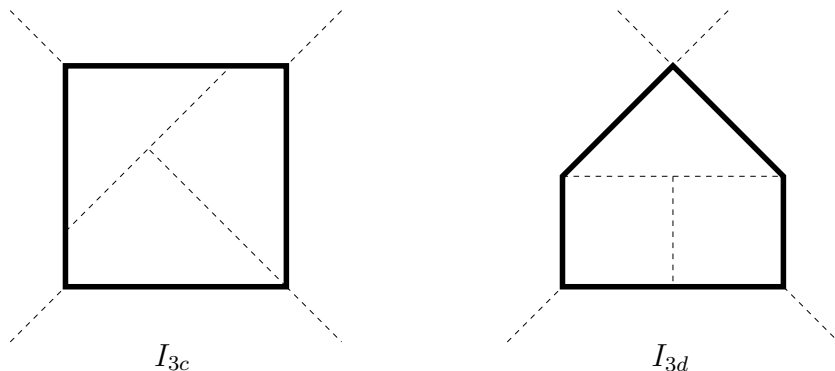

Figure 4: Three-loop four-point dual conformal diagrams, with numerator factors omitted. Both integrals require a factor of m^2 in the numerator in order to be dual-conformally-invariant.

As discussed in ref. [25], these are consistent with eqs. (3.9) and (3.10) provided

$$\gamma(a) = 4a - 4\zeta_2 a^2 + \mathcal{O}(a^3), \qquad \tilde{\mathcal{G}}_0(a) = -\zeta_3 a^2 + \mathcal{O}(a^3), \qquad \tilde{c}(a) = \frac{\pi^4}{120}a^2 + \mathcal{O}(a^3). \quad (3.15)$$

The expression for $\gamma(a)$ is consistent with eq. (3.3).

We now test exponentiation (3.8) at the three-loop level, i.e., the prediction (3.11). Since an explicit calculation of higher-loop amplitudes using the Higgs regulator is not (yet) available, we will start from the assumption (2.13) that only dual-conformal integrals contribute. Equation (2.13) requires two ingredients: the set of dual-conformal integrals and their coefficients. In order to identify the allowed set of dual conformal integrals it is helpful to use the dual notation and graphs introduced in section 2. (For more details and examples, see refs. [8, 10, 46, 47, 54].)

There are four dual conformal integrals that can in principle appear [54] in a four-point three-loop amplitude: I_{3a}, I_{3b}, I_{3c}, and I_{3d}. The first two, depicted in fig. 3, are natural dual conformal analogs of the integrals appearing in the three-loop amplitude computed in dimensional regularization [2]. The last two, depicted in fig. 4, are absent in dimensional regularization. We will assume that these are the only integrals required in the Higgs regularization, with the same

coefficients as in the dimensional regularization result. In general it is not valid to take a result computed in one regularization and transpose it to a different regularization; here this procedure can be justified *a posteriori* (as we discuss below) by imposing that the IR singular terms of the amplitude obey the relation eq. (3.8) as required on general field theory grounds.[16]

Given these assumptions we write

$$M^{(3)}(s,t) = -\frac{1}{8} \left[I_{3a}(s,t,m^2) + I_{3a}(t,s,m^2) + 2\, I_{3b}(s,t,m^2) + 2\, I_{3b}(t,s,m^2) \right] . \qquad (3.16)$$

In appendix A, Mellin-Barnes (MB) representations for the integrals appearing in eq. (3.16) are derived. The small m^2 limit of these MB integrals is extracted using the same method as in ref. [25]. At the kinematic point $s = t$, we find

$$\begin{aligned} I_{3a}(x) &= \frac{17}{90} \log^6(x) + \frac{1}{9}\pi^2 \log^4(x) - \frac{8}{3}\zeta_3 \log^3(x) \qquad\qquad (3.17) \\ &\quad -64.93939402 \log^2(x) - 200.29103 \log(x) - 196.597 + \mathcal{O}(x) , \\ I_{3b}(x) &= \frac{43}{180} \log^6(x) - \frac{2}{9}\pi^2 \log^4(x) - \frac{8}{3}\zeta_3 \log^3(x) \qquad\qquad (3.18) \\ &\quad +37.8813132 \log^2(x) + 113.11769 \log(x) + 90.0915 + \mathcal{O}(x) , \end{aligned}$$

where the decimal coefficients are approximations obtained by numerical integration of MB integrals. We find that the three-loop amplitude (3.16) at $s = t$ is consistent with the exponential ansatz (3.11) provided that

$$\gamma^{(3)} \approx 23.81111114 \pm 10^{-8}, \qquad \tilde{\mathcal{G}}_0^{(3)} \approx 2.68887 \pm 10^{-5}, \qquad \tilde{c}^{(3)} \approx -9.249 \pm 10^{-3} . \qquad (3.19)$$

together with eq. (3.15). We note that $\gamma^{(3)} \approx 22\zeta_4$ is indeed the correct three-loop cusp anomalous dimension (3.3).

Having obtained the coefficients from the $s = t$ case, we are now in a position to test the full consistency of eq. (3.16) with eq. (3.11). In order to do this, we have evaluated the coefficients of the small m^2 expansion of the integrals I_{3a} and I_{3b} numerically for various values of the kinematical variables s, t. We have found agreement with eq. (3.11) within the numerical accuracy of the calculation.

We assumed above that the coefficients of the integrals I_{3c} and I_{3d} vanish in Higgs regularization, as they do in dimensional regularization. We have nevertheless evaluated these integrals in the small m^2 limit using MB methods, and found that

$$\begin{aligned} I_{3c}(u,v) &= 56.23 + \mathcal{O}(m^2) \qquad\qquad\qquad\qquad (3.20) \\ I_{3d}(u,v) &= -17.32 \log(v) - 62 + \mathcal{O}(m^2) \qquad\qquad (3.21) \end{aligned}$$

so that, if present, they could be simply accommodated in the BDS ansatz at three loops by redefining[17] $\tilde{\mathcal{G}}_0^{(3)}$ and $\tilde{c}^{(3)}$ in eq. (3.11). We will therefore not discuss them further in this paper.

---

[16]It would be desirable to determine the coefficients of these integrals using a unitarity-based method. Indeed, once a basis of integrals has been established, in our case using dual conformal symmetry, (generalized) unitarity cuts are a powerful tool to compute the coefficients of the integrals (see e.g. refs. [47, 55–58]).

[17]Such a change could be detected when checking eq. (3.8) at higher orders in perturbation theory.

Equation (3.11) predicts the three-loop amplitude for arbitrary values of u and v. We would like to present a further test of eq. (3.11) in the limit $s \gg t$, i.e. $u \ll v$. This is Regge limit (a) discussed in the introduction. In order to find formulas for our integrals in Regge limit (a), we perform the small m^2 and subsequently the $u \ll v$ limit in the MB integrals. In this way, we obtain an expression in terms of powers of $\log(u)$ and $\log(v)$, whose kinematic-independent coefficients are either numbers or (relatively simple) MB integrals. Where necessary we evaluate the latter numerically.

Let us first collect the results for the one- and two-loop diagrams [25]. The one-loop box diagram gives

$$\lim_{u \ll v} \lim_{u,v \ll 1} I_1(u,v) = \log(u) \left[2 \log(v) + \mathcal{O}(v) \right] + \left[-\pi^2 + \mathcal{O}(v) \right] + \mathcal{O}(u). \tag{3.22}$$

For the two-loop horizontal ladder diagram (cf. fig. 3), one has

$$
\begin{aligned}
\lim_{u \ll v} \lim_{u,v \ll 1} I_2(u,v) &= \log(u) \left[\frac{4}{3} \log^3(v) + \frac{4}{3} \pi^2 \log(v) + \mathcal{O}(v) \right] \\
&+ \left[-\frac{1}{3} \log^4(v) - 2\pi^2 \log^2(v) - 4\zeta_3 \log(v) - \frac{7}{15} \pi^4 + \mathcal{O}(v) \right] + \mathcal{O}(u),
\end{aligned}
\tag{3.23}
$$

while for the two-loop vertical ladder

$$
\begin{aligned}
\lim_{u \ll v} \lim_{u,v \ll 1} I_2(v,u) &= \log^2(u) \left[2 \log^2(v) + \mathcal{O}(v) \right] \\
&+ \log(u) \left[-\frac{4}{3} \log^3(v) - \frac{8}{3} \pi^2 \log(v) - 4\zeta_3 + \mathcal{O}(v) \right] \\
&+ \left[\frac{1}{3} \log^4(v) + 2\pi^2 \log^2(v) + \frac{2}{3} \pi^4 + \mathcal{O}(v) \right] + \mathcal{O}(u).
\end{aligned}
\tag{3.24}
$$

Substituting these results into eq. (3.12), we find agreement with eqs. (3.9) and (3.10) with the coefficients given in eq. (3.15). (The limit $u \ll v$ does not affect the form of eqs. (3.9) and (3.10).)

We now turn to the three-loop diagrams. For the three-loop horizontal ladder diagram (cf. fig. 3), we obtain[18]

$$
\begin{aligned}
\lim_{u \ll v} \lim_{u,v \ll 1} I_{3a}(u,v) &= \log(u) \left[\frac{4}{15} \log^5(v) + \frac{8}{9} \pi^2 \log^3(v) + \frac{28}{45} \pi^4 \log(v) + \mathcal{O}(v) \right] \\
&+ \left[-\frac{7}{90} \log^6(v) - \frac{7}{9} \pi^2 \log^4(v) - \frac{8}{3} \zeta_3 \log^3(v) - \frac{58}{45} \pi^4 \log^2(v) - 35.786 \log(v) - 323.7 + \mathcal{O}(v) \right] \\
&+ \mathcal{O}(u),
\end{aligned}
\tag{3.25}
$$

---

[18]The coefficients of the π^4 terms were obtained numerically, and replaced by their probable rational equivalents.

while for the vertical three-loop ladder, we obtain

$$\lim_{u \ll v} \lim_{u,v \ll 1} \quad I_{3a}(v, u) = \log^6(u) \left[\frac{1}{90} + \mathcal{O}(v) \right] + \log^5(u) \left[-\frac{2}{15} \log(v) + \mathcal{O}(v) \right]$$

$$+ \log^4(u) \left[\frac{2}{3} \log^2(v) + \frac{2}{9} \pi^2 + \mathcal{O}(v) \right] + \log^3(u) \left[-\frac{4}{9} \log^3(v) - \frac{16}{9} \pi^2 \log(v) + O(v) \right]$$

$$+ \log^2(u) \left[2\pi^2 \log^2(v) - 8\zeta_3 \log(v) + \frac{44}{45} \pi^4 + \mathcal{O}(v) \right] \tag{3.26}$$

$$+ \log(u) \left[\frac{2}{15} \log^5(v) + 8\zeta_3 \log^2(v) - \frac{74}{45} \pi^4 \log(v) + 75.717 + \mathcal{O}(v) \right]$$

$$+ \left[-\frac{2}{45} \log^6(v) - \frac{1}{3} \pi^2 \log^4(v) - \frac{8}{3} \zeta_3 \log^3(v) - 111.5 \log(v) + 141.2 + \mathcal{O}(v) \right] + \mathcal{O}(u) \,.$$

For the tennis court diagram in the orientation shown in fig. 3 we find,

$$\lim_{u \ll v} \lim_{u,v \ll 1} \quad I_{3b}(u, v) = \log^6(u) \left[-\frac{1}{90} + \mathcal{O}(v) \right] + \log^5(u) \left[\frac{2}{15} \log(v) + \mathcal{O}(v) \right]$$

$$+ \log^4(u) \left[-\frac{2}{3} \log^2(v) - \frac{2}{9} \pi^2 + \mathcal{O}(v) \right] + \log^3(u) \left[\frac{16}{9} \log^3(v) + \frac{16}{9} \pi^2 \log(v) + O(v) \right]$$

$$+ \log^2(u) \left[-\frac{4}{3} \log^4(v) - 4\pi^2 \log^2(v) - \frac{44}{45} \pi^4 + \mathcal{O}(v) \right] \tag{3.27}$$

$$+ \log(u) \left[\frac{1}{3} \log^5(v) + \frac{20}{9} \pi^2 \log^3(v) - 8\zeta_3 \log^2(v) + \frac{20}{9} \pi^4 \log(v) - 24.8863 + \mathcal{O}(v) \right]$$

$$+ \left[\frac{1}{180} \log^6(v) + \frac{16}{3} \zeta_3 \log^3(v) - \frac{13}{45} \pi^4 \log^2(v) + 111.499 \log(v) - 206.1 + \mathcal{O}(v) \right] + \mathcal{O}(u) \,,$$

while for the tennis court in the transposed orientation, we obtain

$$\lim_{u \ll v} \lim_{u,v \ll 1} \quad I_{3b}(v, u) = \log^6(u) \left[\frac{1}{180} + \mathcal{O}(v) \right] + \log^5(u) \left[-\frac{1}{15} \log(v) + \mathcal{O}(v) \right]$$

$$+ \log^4(u) \left[\frac{1}{3} \log^2(v) + \frac{1}{9} \pi^2 + \mathcal{O}(v) \right] + \log^3(u) \left[-\frac{8}{9} \log^3(v) - \frac{8}{9} \pi^2 \log(v) + O(v) \right]$$

$$+ \log^2(u) \left[\frac{4}{3} \log^4(v) + \frac{8}{3} \pi^2 \log^2(v) + \frac{22}{45} \pi^4 + \mathcal{O}(v) \right] \tag{3.28}$$

$$+ \log(u) \left[-\frac{8}{15} \log^5(v) - \frac{8}{3} \pi^2 \log^3(v) - \frac{8}{5} \pi^4 \log(v) + \mathcal{O}(v) \right]$$

$$+ \left[\frac{1}{18} \log^6(v) + \frac{5}{9} \pi^2 \log^4(v) - \frac{8}{3} \zeta_3 \log^3(v) + \frac{14}{15} \pi^4 \log^2(v) - 24.888 \log(v) + 280.8 + \mathcal{O}(v) \right]$$

$$+ \mathcal{O}(u) \,.$$

Plugging these into eq. (3.11), we see that the $\log^6(u), \log^5(u)$, and $\log^4(u)$ terms cancel, and that the $\log^3(u)$, $\log^2(u)$, $\log(u)$, and $\log^0(u)$ terms of eq. (3.11) are reproduced using the coefficients given in eqs. (3.15) and (3.19).

In summary, we used the assumption of extended dual conformal symmetry to restrict the integrals allowed to appear in the three-loop four-point amplitude to I_{3a}, I_{3b}, I_{3c}, and I_{3d}. We then successfully checked the consistency of this assumption with the exponential ansatz (3.11). The first test consisted in computing the small m^2 expansion of the amplitude, and numerically comparing to eq. (3.11) for various values of the kinematical variables u and v. The second test consisted in comparing our result to eq. (3.11) in the limit $u \ll v$.

4   Regge limit of the four-gluon amplitude

In this section, we examine the four-point amplitude $M(s,t)$ in the Regge limit $s \gg t > 0$. (Recall that $M(s,t)$ is real in this kinematic region (see footnote 9). The "physical" Regge limit, $-s \gg t > 0$, differs from this by an imaginary contribution.) First we review the situation for dimensional regularization, and then we reexamine the Regge limit using Higgs regularization and cutoff regularization. The divergence structure of the Regge limit can also be understood via the scattering of massive particles.

4.1   Regge limit in dimensional regularization

We recall that in dimensional regularization the Regge form of $M(s,t)$ is [10, 30–32]

$$M(s,t) = \beta(t) \left(\frac{s}{t}\right)^{\alpha(t)-1} \tag{4.1}$$

where the trajectory function is[19]

$$\alpha(t) - 1 \;\; = \;\; \sum_{\ell=1}^{\infty} a^{\ell} \left[\frac{\gamma^{(\ell)}}{4\ell\epsilon} + \frac{\mathcal{G}_0^{(\ell)}}{2}\right] \left(\frac{\mu^2}{t}\right)^{\ell\epsilon} + \mathcal{O}(\epsilon) \tag{4.2}$$

and the form of the residue $\beta(t)$ may be found in ref. [30, 32].

The form of eq. (4.1) suggests that the IR-finite contribution to the L-loop amplitude $M^{(L)}(s,t)$ grows as $\log^L(s)$ in the Regge limit. This conclusion, however, is not quite warranted because the neglected $\mathcal{O}(\epsilon)$ and higher terms could in principle conspire with the pole terms to yield higher powers of $\log(s)$. Nevertheless, it was shown that this does not occur at least through three loops [32], and that the L-loop amplitude in fact grows as $\log^L(s)$. It is not unreasonable to hope that this should hold to all orders.

On the other hand, it is definitely not true that the individual L-loop diagrams contributing to $M^{(L)}(s,t)$ are bounded by $\log^L(s)$ in the Regge limit. As an explicit counterexample, consider the Regge limit of the contributions to the three-loop amplitude, keeping only terms of order

---

[19]The tree amplitude supplies another power of s/t so that, in the Regge limit, the color-ordered amplitude $A(p_i, \varepsilon_i)$ goes as $(s/t)^{\alpha(t)}$.

$\log^3(s/t)$ or higher:

$$I_{3a}(s,t) = \mathcal{O}(\mathcal{L}), \tag{4.3}$$

$$I_{3a}(t,s) = \left(\frac{\mu^2}{t}\right)^{3\epsilon}\left[\frac{1}{\epsilon^3}\left(-\mathcal{L}^3\right) + \frac{1}{\epsilon^2}\left(\frac{1}{12}\mathcal{L}^4\right) + \frac{1}{\epsilon}\left(\frac{1}{60}\mathcal{L}^5 + \frac{25\pi^2}{36}\mathcal{L}^3\right) + \mathcal{O}(\epsilon^0)\right] + \mathcal{O}(\mathcal{L}^2),$$

$$I_{3b}(s,t) = \left(\frac{\mu^2}{t}\right)^{3\epsilon}\left[\frac{1}{\epsilon^3}\left(-\frac{1}{3}\mathcal{L}^3\right) + \frac{1}{\epsilon^2}\left(-\frac{1}{12}\mathcal{L}^4\right) + \frac{1}{\epsilon}\left(-\frac{1}{60}\mathcal{L}^5 - \frac{13\pi^2}{36}\mathcal{L}^3\right) + \mathcal{O}(\epsilon^0)\right] + \mathcal{O}(\mathcal{L}^2),$$

$$I_{3b}(t,s) = \left(\frac{\mu^2}{t}\right)^{3\epsilon}\left[\frac{1}{\epsilon^3}\left(\frac{1}{6}\mathcal{L}^3\right) + \frac{1}{\epsilon^2}\left(\frac{1}{24}\mathcal{L}^4\right) + \frac{1}{\epsilon}\left(\frac{1}{120}\mathcal{L}^5 + \frac{13\pi^2}{72}\mathcal{L}^3\right) + \mathcal{O}(\epsilon^0)\right] + \mathcal{O}(\mathcal{L}^2)$$

where we have denoted $\mathcal{L} \equiv \log(s/t)$. Combining these contributions using eq. (3.16), we obtain the Regge limit of the three-loop amplitude

$$M^{(3)}(s,t) = \left(\frac{\mu^2}{t}\right)^{3\epsilon}\left[\frac{1}{6\epsilon^3} - \frac{\pi^2}{24\epsilon} + \mathcal{O}(\epsilon^0)\right]\mathcal{L}^3 + \mathcal{O}(\mathcal{L}^2) \tag{4.4}$$

but it is clear that the Regge behavior comes from no single diagram, and in fact a cancellation of higher powers of $\log(s/t)$ occurs among the various contributing diagrams. This means that in dimensional regularization, it is very difficult to ascertain the Regge behavior of $M^{(L)}(s,t)$ by considering the Regge behavior of individual diagrams.

In the next section, we will compare this to the Regge limit in Higgs regularization. As was noted in the introduction, there is a subtlety, namely that the Regge limit of individual diagrams can depend on the order in which the various limits are taken. As we will see in the next section, with one way of taking the limits, the leading Regge behavior of the L-loop amplitude is determined by a single contributing diagram, the vertical ladder diagram.

4.2 Regge limit in Higgs regularization

The conjectured exponentiation eq. (3.8) of the four-point amplitude in Higgs regularization can be rewritten as

$$\log M(s,t) = -\frac{1}{4}\gamma(a)\log\left(\frac{t}{m^2}\right)\log\left(\frac{s}{m^2}\right) - \tilde{\mathcal{G}}_0(a)\left[\log\left(\frac{t}{m^2}\right) + \log\left(\frac{s}{m^2}\right)\right] + \frac{\pi^2}{8}\gamma(a) + \tilde{c}(a) + \mathcal{O}(m^2) \tag{4.5}$$

As pointed out in sec. 3, in Higgs regularization we may simply exponentiate eq. (4.5) to obtain the four-point amplitude. Moreover, eq. (4.5) implies that the amplitude is Regge exact,[20] up to terms that vanish as $m^2 \to 0$:

$$M(s,t) = \beta(t)\left(\frac{s}{m^2}\right)^{\alpha(t)-1} + \mathcal{O}(m^2) \tag{4.6}$$

---

[20] Equation (4.6) could also be rewritten with s and t exchanged, due to the $s \leftrightarrow t$ symmetry of eq. (4.5).

with

$$\alpha(t) - 1 \;=\; -\frac{1}{4}\gamma(a)\log\!\left(\frac{t}{m^2}\right) - \tilde{\mathcal{G}}_0(a)\,, \tag{4.7}$$

$$\beta(t) \;=\; \exp\left[-\tilde{\mathcal{G}}_0(a)\log\!\left(\frac{t}{m^2}\right) + \frac{\pi^2}{8}\gamma(a) + \tilde{c}(a)\right]. \tag{4.8}$$

The $-\frac{1}{4}\gamma(a)\log(t/m^2)$ piece of the trajectory $\alpha(t)$ agrees with the conjecture in eq. (2.18) of ref. [41], but in addition there is a contribution from the analog of the collinear anomalous dimension.

Equation (4.5) implies that the leading-log (LL) behavior of the L-loop amplitude is given by

$$M^{(L)}(s,t) \;\xrightarrow[s\gg t]{}\; \frac{(-1)^L}{L!}\log^L\!\left(\frac{t}{m^2}\right)\log^L\!\left(\frac{s}{m^2}\right). \tag{4.9}$$

In fact we can use eq. (4.5) to organize the L-loop amplitude in a leading-log expansion in $\log(s/m^2)$, with LL, NLL, and NNLL terms given by (recalling that $u \equiv m^2/s$ and $v \equiv m^2/t$)

$$
\begin{aligned}
M^{(L)} \;=\; & \left[\frac{1}{L!}(-\log v)^L\right]\log^L(u) \\
+\; & \left[\left(\frac{\pi^2}{2(L-1)!} + \frac{\gamma^{(2)}}{4(L-2)!}\right)(-\log v)^{L-1} + \frac{\tilde{\mathcal{G}}_0^{(2)}}{(L-2)!}(-\log v)^{L-2}\right]\log^{L-1}(u) \\
+\; & \left[-\frac{\tilde{\mathcal{G}}_0^{(2)}}{(L-2)!}(-\log v)^{L-1}\right. \\
+\; & \left(\frac{8\tilde{c}^{(2)} + \pi^4 + \pi^2\gamma^{(2)}}{8(L-2)!} + \frac{2\gamma^{(3)} + \pi^2\gamma^{(2)}}{8(L-3)!} + \frac{(\gamma^{(2)})^2}{32(L-4)!}\right)(-\log v)^{L-2} \\
+\; & \left.\left(\frac{2\tilde{\mathcal{G}}_0^{(3)} + \pi^2\tilde{\mathcal{G}}_0^{(2)}}{2(L-3)!} + \frac{\gamma^{(2)}\tilde{\mathcal{G}}_0^{(2)}}{4(L-4)!}\right)(-\log v)^{L-3} + \frac{(\tilde{\mathcal{G}}_0^{(2)})^2}{2(L-4)!}(-\log v)^{L-4}\right]\log^{L-2}(u) \\
+\; & \mathcal{O}(\log^{L-3}(u)) \tag{4.10}
\end{aligned}
$$

where we have explicitly set $\gamma^{(1)} = 4$ and $\tilde{\mathcal{G}}_0^{(1)} = \tilde{c}^{(1)} = 0$. In fact we have already tested the validity of this expansion through three loops in sec. 3 by evaluating the integrals that contribute to the amplitudes in a leading log expansion.

As discussed in the introduction, however, there is a subtlety in how one evaluates the leading log expansion of the integrals contributing to the four-point amplitude. One approach, which we term (a), is to first evaluate all the integrals in the small m^2 limit, and subsequently to take the limit $s \gg t$. This is what has been done for all integrals up to this point in the paper. In this section, we will explore another approach, which we call (b), in which we evaluate the $s \gg t$ limit of the integrals first, for finite m^2, and subsequently take the small m^2 limit of the coefficients of the leading log expansion. We will find that, although the intermediate details differ, the final result is still given (at least through three loops) by eq. (4.10).

19

For one and two loops, we have verified that both methods (a) and (b) yield the same results for the integrals namely, eqs. (3.22), (3.23), and (3.24). At three loops, however, the results begin to differ. The three-loop horizontal ladder diagram (cf. fig. 3), gives[21]

$$\lim_{u,v\ll1}\lim_{u\ll v} \ I_{3a}(u,v) = \log(u)\left[\frac{4}{15}\log^5(v) + \frac{8}{9}\pi^2\log^3(v) + \frac{28}{45}\pi^4\log(v) + \mathcal{O}(v)\right] \tag{4.11}$$

$$+ \ \left[-\frac{7}{90}\log^6(v) - \frac{7}{9}\pi^2\log^4(v) - \frac{8}{3}\zeta_3\log^3(v) + \frac{58}{45}\pi^4\log^2(v) - 35.786\log(v) - 323.7 + \mathcal{O}(v)\right]$$

$$+ \ \mathcal{O}(u),$$

which in fact agrees with eq. (3.25). The vertical three-loop ladder, however, gives in the (b) limit

$$\lim_{u,v\ll1}\lim_{u\ll v} \ I_{3a}(v,u) = \log^3(u) \ \left[\frac{4}{3}\log^3(v) + \mathcal{O}(v)\right] \tag{4.12}$$

$$+ \ \log^2(u) \ \left[-\frac{8}{3}\log^4(v) - \frac{10}{3}\pi^2\log^2(v) - 8\zeta_3\log(v) + \mathcal{O}(v)\right]$$

$$+ \ \log(u) \ \left[\frac{34}{15}\log^5(v) + \frac{64}{9}\pi^2\log^3(v) + 8\zeta_3\log^2(v) + \frac{34}{15}\pi^4\log(v) + 75.717 + \mathcal{O}(v)\right]$$

$$+ \ \left[-\frac{34}{45}\log^6(v) - \frac{35}{9}\pi^2\log^4(v) - \frac{8}{3}\zeta_3\log^3(v) - \frac{176}{45}\pi^4\log^2(v) - 111.504\log(v) - 363.4 + \mathcal{O}(v)\right]$$

$$+ \ \mathcal{O}(u).$$

In the other way (a) of taking the limit, the leading term goes as $\log^6(u)$. For the tennis court diagram in the orientation shown in fig. 3 we obtain

$$\lim_{u,v\ll1}\lim_{u\ll v} \ I_{3b}(u,v) = \log^2(u) \ \left[\frac{4}{3}\log^4(v) + \frac{4}{3}\pi^2\log^2(v) + \mathcal{O}(v)\right] \tag{4.13}$$

$$+ \ \log(u) \ \left[-\frac{9}{5}\log^5(v) - \frac{44}{9}\pi^2\log^3(v) - 8\zeta_3\log^2(v) - \frac{76}{45}\pi^4\log(v) - 24.886 + \mathcal{O}(v)\right]$$

$$+ \ \left[\frac{43}{60}\log^6(v) + \frac{32}{9}\pi^2\log^4(v) + \frac{16}{3}\zeta_3\log^3(v) - \frac{143}{45}\pi^4\log^2(v) + 111.499\log(v) + 298.5 + \mathcal{O}(v)\right]$$

$$+ \ \mathcal{O}(u),$$

while for the tennis court in the transposed orientation, we obtain

$$\lim_{u,v\ll1}\lim_{u\ll v} \ I_{3b}(v,u) = \log(u) \ \left[\frac{8}{15}\log^5(v) + \frac{8}{9}\pi^2\log^3(v) + \frac{16}{45}\pi^4\log(v) + \mathcal{O}(v)\right] \tag{4.14}$$

$$+ \ \left[-\frac{3}{10}\log^6(v) - \frac{11}{9}\pi^2\log^4(v) - \frac{8}{3}\zeta_3\log^3(v) - \frac{46}{45}\pi^4\log^2(v) - 24.888\log(v) + 28.5 + \mathcal{O}(v)\right]$$

$$+ \ \mathcal{O}(u).$$

---

[21]The coefficients of the π^4 terms were obtained numerically, and replaced by their probable rational equivalents.

Thus, the form of the leading log expansion of the three-loop integrals depends on the order in which the limits are taken.

Despite the different expressions for the individual integrals, we find that the three-loop amplitude itself is the same in both Regge (a) and (b) limits. Plugging the expressions above into eq. (3.16), we find that the expression (3.11) is reproduced, using the coefficients in eqs. (3.15) and (3.19), just as when we evaluated the integrals in the other order of limits. In sec. 4.4, we give an heuristic argument which helps to explain why the Regge limit of the amplitude should be independent of the order in which the limits are taken.

A significant difference between these two approaches is that while, in the Regge (a) limit, most of the diagrams contribute to the leading log term (4.9) of the amplitude (as is also the case in dimensional regularization), in the Regge (b) limit, only one diagram, the vertical ladder, contributes to the leading-log behavior of the amplitude in the Regge limit. Using

$$M^{(L)} = \left(-\frac{1}{2} \right)^L \left[I_{La}(v, u) + \quad (\text{all other } L-\text{loop diagrams}) \ \right] \tag{4.15}$$

one can show that the leading log behavior of the L-loop amplitude (4.9) can be wholly accounted for by the vertical L-loop ladder diagram $I_{La}(v, u)$, suggesting that all other diagrams are subdominant (i.e., grow no faster than $\log^{L-1}(s)$) in the Regge (b) limit. Using the methods of ref. [35], we derive in appendix C the LL, NLL, and NNLL contributions of the vertical L-loop diagram, obtaining

$$\lim_{u,v \ll 1} \lim_{u \ll v} \ I_{La}(v, u) = \frac{2^L}{L!} \log^L u \log^L v$$

$$- \frac{2^L}{(L-1)!} \log^{L-1} u \left[\frac{1}{3}(L-1)\log^{L+1} v + (L+2)\zeta_2 \log^{L-1} v + (L-1)\zeta_3 \log^{L-2} v \right]$$

$$+ \frac{2^L}{(L-2)!} \log^{L-2} u \left[\frac{10L^2 - 14L + 3}{180} \log^{L+2} v + \frac{(L+1)^2}{18} \pi^2 \log^L v \right.$$

$$+ \frac{L(L-2)}{3} \zeta_3 \log^{L-1} v + \frac{(L+3)(5L+2)}{360} \pi^4 \log^{L-2} v + \frac{L-2}{6}(L+1.826)\pi^2 \zeta_3 \log^{L-3} v$$

$$+ \left. \frac{(L-2)(L-3)}{2} \zeta_3^2 \log^{L-4} v \right] + \mathcal{O}(\log^{L-3} u) . \tag{4.16}$$

It is clear from comparing eqs. (4.10) and (4.16) that other diagrams begin to contribute at the NLL order. It is difficult, however, to use the methods of ref. [35] to estimate the leading logarithmic growth for the other diagrams due to the presence of numerator factors in the integrals. (It would be interesting to extend the methods of ref. [35] to these cases.) We suspect that only a small subset of the allowed L-loop diagrams contribute to the NLL terms of $M^{(L)}$; it would be nice to characterize which.

4.3   Regge limit in cutoff regularization

Mandelstam [59] has given certain criteria for establishing whether Reggeization occurs, i.e. whether an elementary field in a Lagrangian field theory lies on a Regge trajectory or not. It

depends on a "counting procedure," which must be carried out separately for each field of the Lagrangian, where for renormalizable theories one simply does the counting at $j = 0, 1/2$, or 1 to consider the issue. It has been shown [60–62] that the elementary fields of renormalizable Yang-Mills gauge theories lie on a Regge trajectory if the theory has a mass gap, where theories with a Higgs mechanism provide a case in point. These arguments are purely local in nature, in that the trajectory of a gluon passes through $j = 1$ at the mass of the particle, but no global information about the trajectory is provided in this construction.

In addition to the "counting criteria," a certain factorization condition among the helicity matrices of the scattering process must be satisfied if the Reggeization is to take place. This requirement results from the solution of the unitarity-analyticity equations satisfied by the scattering amplitude analytically continued in angular momentum. As a result an integral equation must be satisfied, where the potential V is the inhomogeneous term in the integral equation. If V is taken to be the kinematical-singularity-free, partial-wave projection of the Born approximation helicity amplitude, the solution to the integral equation provides an analytic form for the Regge trajectory which is equivalent to the LL approximation to the trajectory function.[22]

Given this background, in ref. [41] the Regge limit of the ladder approximation for the color-ordered, tree-approximation-stripped amplitude was considered, with cutoff regularization (i.e., all the propagators in the loop integrals are given a mass m) for gluon-gluon scattering in $\mathcal{N} = 4$ SYM. It was shown that

$$M(s,t) \quad \xrightarrow[s \gg t]{} \quad \beta(t) \left(\frac{s}{m^2}\right)^{\alpha(t)-1}, \tag{4.17}$$

where

$$\alpha(t) = 1 - a \log\left(\frac{t}{m^2}\right) + \mathcal{O}(a^2). \tag{4.18}$$

Hence eq. (4.18) agrees with eq. (4.8) to lowest order in the coupling. The reason for this is that, as we saw above, (1) the leading log contribution to the L-loop amplitude in the Regge (b) limit in Higgs regularization comes from the vertical ladder diagram alone, and (2) as we show in appendix C, the LL contribution of the vertical ladder is independent of the masses of the propagators of the rungs of the ladder, which is the only difference between the Higgs- and cutoff-regulated diagrams.

In ref. [41] it was conjectured that with the cutoff regularization

$$\alpha(t) = 1 - \frac{1}{4}\gamma(a) \log\left(\frac{t}{m^2}\right), \tag{4.19}$$

which satisfies

$$\alpha(m^2) = 1, \tag{4.20}$$

as required by general principles. Note that eq. (4.19) coincides with eq. (4.8) from the Higgs regularization up to a scheme-dependent constant, which begins at $\mathcal{O}(a^2)$.

While Higgs and cutoff regulators yield identical results at the leading log level, one could ask whether they differ at the subleading log level. Consider the diagrams that contribute to the two-loop amplitude (3.12). Whereas in Higgs-regularization the middle line is massless, in the cutoff

---

[22]See sec. 2 of ref. [63].

scheme, all internal propagators have a uniform mass m.[23] To compute the two-loop diagram with uniformly massive propagators, more MB integrals are needed relative to the Higgs-regulated case. For example, a naive use of AMBRE [64] yields a nine-fold MB representation. Using the methods described in appendix A, we have written down a seven-fold MB representation, from which we extract the following results in the Regge (b) limit $u \ll v \ll 1$:

$$\lim_{u,v \ll 1} \lim_{u \ll v} I_{2;\,\mathrm{cutoff}}(u,v) = \log(u) \left[\frac{4}{3} \log^3(v) + \frac{4}{3} \pi^2 \log(v) + 4\zeta_3 + \mathcal{O}(v) \right] + \mathcal{O}(\log^0(u)),$$

$$\lim_{u,v \ll 1} \lim_{u \ll v} I_{2;\,\mathrm{cutoff}}(v,u) = \log^2(u) \left[2 \log^2(v) + O(v) \right] \qquad (4.21)$$

$$+ \log(u) \left[-\frac{4}{3} \log^3(v) - \frac{8}{3} \pi^2 \log(v) + \frac{4}{3} \zeta_3 + \mathcal{O}(v) \right] + \mathcal{O}(\log^0(u)).$$

Comparing this with eqs. (3.23) and (3.24), we see that the ζ_3 coefficients in the $\log(u)$ terms are changed. There are presumably also changes in the uncomputed $\log^0(u)$ terms.

We can also compute the NLL terms of the cutoff-regulated L-loop vertical ladder diagram. The calculation of appendix C is unchanged, except that the middle rungs of the $(2 + 2\epsilon)$-dimensional diagrams depicted in fig. 9 become massive. As a result, the integral B_2 in eq. (C.25), for example, is changed to

$$e^{-2\epsilon\gamma_{\mathrm{E}}} B_{2;\,\mathrm{cutoff}} = 4 \log^2 u + \epsilon \left[\frac{10}{3} \log^3 u + \frac{4}{3} \pi^2 \log u - \frac{4}{3} \zeta_3 \right] + \dots \qquad (4.22)$$

as a consequence of which we have

$$\lim_{u,v \ll 1} \lim_{u \ll v} I_{La;\,\mathrm{cutoff}}(v,u) = \frac{2^L}{L!} \log^L u \log^L v$$

$$- \frac{2^L}{(L-1)!} \log^{L-1} u \left[\frac{1}{3}(L-1) \log^{L+1} v + (L+2)\zeta_2 \log^{L-1} v - \frac{1}{3}(L-1)\zeta_3 \log^{L-2} v \right]$$

$$+ \mathcal{O}(\log^{L-2} u) \qquad (4.23)$$

which should be compared with eq. (4.16).

4.4 Scattering of massive particles and Regge behavior

In this section, we present a different approach which helps to explain why we obtained the same three-loop amplitude from eq. (3.16) in both Regge (a) and (b) limits, despite the fact that the contributing integrals (3.25-3.28) and (4.11-4.14) differ so drastically from one another.

Consider the four-point amplitude on the Coulomb branch of $\mathcal{N} = 4$ SYM theory, as reviewed in sec. 2, with the scattered particles satisfying the on-shell conditions

$$p_i^2 = -(m_i - m_{i+1})^2. \qquad (4.24)$$

---

[23]Note that, in contrast with dimensional or Higgs regularization, it is not clear whether other integrals might not also contribute in cutoff-regularization, as could happen when one goes off-shell.
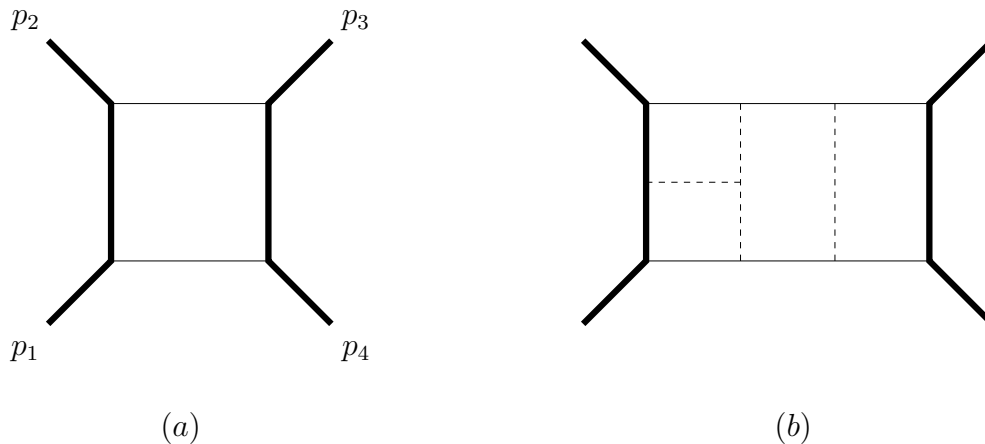
Figure 5: (a) One-loop scattering of massive particles. (b) Sample higher-loop diagram. Fat lines and thin lines denote particles of mass M and m, respectively. Dashed thin lines denote massless particles.

Recall that the assumption of dual conformal symmetry implies that the amplitude is a function of two variables u and v, defined in eq. (2.12). In previous sections of this paper, we considered the equal mass case, $m_i = m$, so that $u = m^2/s$ and $v = m^2/t$, and the external states are massless $p_i^2 = 0$. The Regge limit $s \gg t \gg m^2$ corresponds to $u \ll v \ll 1$.

In this section, we consider instead the two mass case, $m_1 = m_3 = m$ and $m_2 = m_4 = M$, which implies $p_i^2 = -(M - m)^2$, and (cf. eq. (2.12))

$$u = \frac{m^2}{s} \qquad \text{and} \qquad v = \frac{M^2}{t}. \tag{4.25}$$

Dual conformal symmetry implies that the Regge limit $u \ll v \ll 1$ can be attained by choosing $m^2 \ll M^2 \ll s, t$, so that the on-shell condition becomes $p_i^2 \approx -M^2$. This corresponds to the scattering of particles of mass M by the exchange of particles of much lighter mass m. See fig. 5(a) for the one-loop contribution to this scattering. At higher loops, massless particles will also be exchanged in the interior of the diagram; see fig. 5(b) for a sample higher-loop diagram.

As was discussed in the introduction and in section 4 it is important to specify in which order the Regge limit is taken. In this section, we will first take m^2 small for fixed M^2, s, and t. This corresponds to the first part of Regge limit (b), namely, $u \to 0$, i.e., $u \ll v$ and $u \ll 1$. Later in this section, we will take $M^2 \ll s, t$, which corresponds to the second part ($v \ll 1$). The amplitudes discussed above have soft IR divergences (as $m \to 0$), but no collinear divergences, so the double logarithms $\log^2(m^2)$ characteristic of overlapping divergences are absent, leaving only single logarithms $\log(m^2)$. At one loop one can show that

$$M^{(1)}(u, v) \quad \underset{u \to 0}{\longrightarrow} \quad -\frac{1}{2}(\log u)\, \Gamma_{\text{cusp}}(a, \theta)\big|_{1-\text{loop}} + \mathcal{O}(u^0) \tag{4.26}$$

where $\Gamma_{\text{cusp}}(a, \theta)$ is the cusp anomalous dimension [65–68] of a Wilson line with a non-light-like cusp, and with θ being the (Minkowskian) cusp angle defined by $\cosh\theta = p_2 \cdot p_3/M^2$. It is

plausible that the leading behavior for all loops is

$$M(u,v) \quad \underset{u \to 0}{\longrightarrow} \quad \exp\left\{ -\frac{1}{2}(\log u)\,\Gamma_{\text{cusp}}(a,\theta) + \mathcal{O}(u^0) \right\}. \tag{4.27}$$

Next, we take the further limit $M^2 \ll t$, i.e., $v \ll 1$. In this limit, the cusp anomalous dimension goes to [69]

$$\Gamma_{\text{cusp}}(a,\theta) \quad \underset{v \to 0}{\longrightarrow} \quad (\log v)\,\Gamma_{\text{cusp}}(a) + \mathcal{O}(v^0), \tag{4.28}$$

where $\theta \approx -\log v$ and $\Gamma_{\text{cusp}}(a) = \gamma(a)/2$. Accepting the conjectured eq. (4.27), one obtains in the Regge limit

$$\lim_{u,v \ll 1} \lim_{u \ll v} \quad M(u,v) = \exp\left\{ -\frac{1}{2}(\log u)(\log v)\Gamma_{\text{cusp}}(a) + \cdots \right\}. \tag{4.29}$$

Since we have taken the limits in the order $u \ll 1$ with v fixed, followed by $v \ll 1$, this is Regge limit (b) as defined in the introduction. Note that we arrive in this way at the same (leading log) result as eq. (4.5), which was obtained in Regge limit (a), i.e., taking $u, v \ll 1$ first, followed by $u \ll v$. This helps to explain why we obtained the same three-loop amplitude from eq. (3.16) in the two Regge limits, despite the fact that the contributing integrals had different forms in these two limits.

It is also noteworthy that eq. (4.29) directly exhibits the single log behavior expected of the Regge limit, without the cancellation of double logs that occurs in taking the Regge limit (4.5) of the exponential ansatz (3.8).

5 Discussion

In this paper we have tested various conjectures and issues related to the Higgs regulator scheme proposed in ref. [25] for $\mathcal{N} = 4$ SYM theory. The assumption of exact dual conformal symmetry enabled us to compute the four-gluon scattering amplitude in the planar limit to three-loop accuracy. Our results are consistent, in various limits, with an analog of the BDS conjecture proposed for the Higgs-regulated four-gluon amplitude, with the same value (to three loops) of the cusp anomalous dimension as that found in dimensional regularization. This is as expected since the cusp anomalous dimension is IR-scheme-independent.

The Regge limit of the four-point function was considered in various IR regulator schemes. It was shown that the leading log behavior of the Regge trajectory is determined by the sum of vertical ladder graphs for the Higgs regulator and for a cut-off regulator.[24] This contrasts with dimensional regularization, where no single set of diagrams dominates at any order of perturbation theory. Further one may associate the perturbative expansion for the cusp anomalous dimension with the NLL, NNLL, $\cdots$ approximations to the gluon Regge trajectory. A particular

---

[24]Here we are referring to the Regge (b) limit, as defined in the paper.

dual conformal mass assignment allows one to obtain directly the single logarithmic behavior of the Regge trajectory, without the necessity of cancellation of $\log^2$ terms.

We also found in the course of this work that Higgs-regulated amplitudes lead to more efficient integral representations (i.e., fewer MB parameters) than more generic (e.g., cutoff-regulated) schemes.

There are several issues deserving further attention. It would be useful to extend the methods of ref. [35] to determine the Regge limits of diagrams involving non-trivial (i.e., loop-momentum-dependent) numerator factors. It would also be interesting to determine whether there is a simple characterization of the subset of L-loop diagrams that contribute to the NLL, NNLL, $\cdots$ terms in the L-loop amplitude in the Regge limit.

Overall, we have seen that the Higgs regulator for planar $\mathcal{N} = 4$ SYM amplitudes has a number of advantages over other regulators.

Acknowledgments

A   Mellin-Barnes representations of the integrals

In this section we derive Mellin-Barnes (MB) representations for the integrals considered in the paper. In doing so we follow the loop-by-loop approach advocated in refs. [72, 73]. In this approach, one successively derives MB representations for one-loop subintegrals. Remarkably, the Higgs masses can be incorporated rather naturally into this procedure.

Tools that we have found useful are the Mathematica packages MB [70] and AMBRE [64]. The latter can also be used to derive MB representations. Of course, one can sometimes find MB representations involving fewer MB integrals by going through the derivation by hand. Since the number of integrals we need is rather small we have followed the latter strategy. We present details of the derivation below, since the essential steps when deriving MB representations for higher-loop or higher-point integrals are the same.

It is interesting to note that using a uniform cut-off (i.e., giving a mass to *all* propagators of the integral) makes the resulting MB representations considerably more intricate, and one needs more MB parameters.

A.1   MB representation for the 3-loop ladder diagram

Let us consider the three-loop ladder depicted in figure 6a,

$$I_{3a} = s^3\, t \int \frac{d^4x_5 d^4x_6 d^4x_7}{(i\pi^2)^3} \left(P_{25,m}\, P_{15,m}\, P_{35,m}\, P_{56}\, P_{36,m}\, P_{16,m}\, P_{67}\, P_{37,m}\, P_{17,m}\, P_{47,m} \right)^{-1}. \quad \text{(A.1)}$$
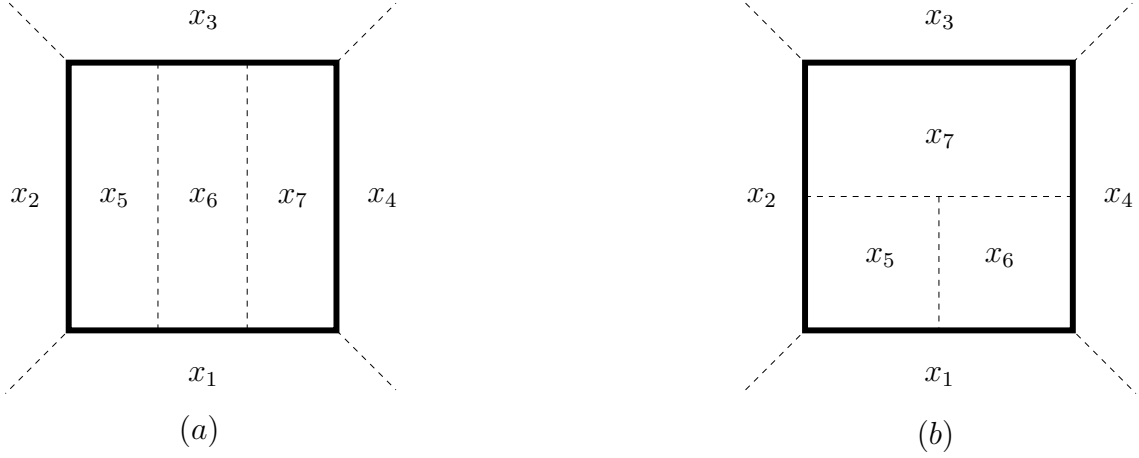
Figure 6: Diagrams of two dual conformal integrals at three loops. Thick lines correspond to massive propagators, thin lines to massless ones. The x_i are dual coordinates. Figure (a) shows the three-loop ladder diagram, with a factor of $s^3 t = (x_{13}^2)^3 x_{24}^2$ removed. Figure (b) shows the tennis court diagram, with a factor of st^2 removed and a numerator $x_{17}^2 + m^2$ not shown in the diagram.

Here $P_{ij,m} = x_{ij}^2 + m^2$ and x_i is the dual notation introduced in sec. 2. In the massless case, it is possible to derive a convenient MB representation by successively doing the loop integrations [72,73]. As we will see presently, the same strategy also works well in the massive case. We begin with the x_5 subintegral

$$I_{3a}^{(1)} \;=\; \int \frac{d^4 x_5}{i\pi^2} \left(P_{15,m} P_{25,m} P_{35,m} P_{56} \right)^{-1} \tag{A.2}$$

where

$$I_{3a} \;=\; s^3 \, t \int \frac{d^4 x_6 d^4 x_7}{(i\pi^2)^2} \, I_{3a}^{(1)} \left(P_{36,m} P_{16,m} P_{67} P_{37,m} P_{17,m} P_{47,m} \right)^{-1} . \tag{A.3}$$

Introducing α parameters (see for example ref. [73]), we obtain

$$I_{3a}^{(1)} \;=\; \int_0^\infty \frac{d\alpha_i \, \delta(\sum \alpha_i - 1)}{[\alpha_1 \alpha_3 s + \alpha_6 \left(\alpha_1 P_{16,m} + \alpha_2 P_{26,m} + \alpha_3 P_{36,m} \right) + (\alpha_1 + \alpha_2 + \alpha_3)^2 m^2]^2} . \tag{A.4}$$

Note that the range of the sum in the delta function can be chosen arbitrarily. Here, it is convenient to choose $\sum_{i=1}^3$ in order to simplify the m^2 term. Performing the α_6 integration, we obtain

$$I_{3a}^{(1)} = \int_0^1 \frac{d\alpha_i \, \delta(\sum_{i=1}^3 \alpha_i - 1)}{(\alpha_1 P_{16,m} + \alpha_2 P_{26,m} + \alpha_3 P_{36,m})(\alpha_1 \alpha_3 s + m^2)} . \tag{A.5}$$

To perform the remaining integrations over the α parameters, we introduce three MB parameters. Using eqs. (A.39) and (A.40), we obtain

$$
\begin{aligned}
I_{3a}^{(1)} \;=\;& \int \frac{dz_i}{(2\pi i)^3} \Gamma(-z_1)\Gamma(-z_2)\Gamma(-z_3)\Gamma(1+z_1+z_3)\Gamma(1+z_2)\,(m^2)^{-1-z_2} \\
& \times \int d\alpha_i\,\delta(\sum_{i=1}^{3}\alpha_i-1)\,(\alpha_1\alpha_3 s)^{z_2}(\alpha_2 P_{26,m})^{-1-z_1-z_3}(\alpha_1 P_{16,m})^{z_1}(\alpha_3 P_{36,m})^{z_3}\,. \quad (A.6)
\end{aligned}
$$

The parameter integrals are now easily done with the help of (A.43), leading to

$$
I_{3a}^{(1)} \;=\; \int \frac{dz_{1,2,3}}{(2\pi i)^3} f^{(1)}(z_1,z_2,z_3)\, s^{z_2}(m^2)^{-1-z_2}(P_{26,m})^{-1-z_1-z_3}(P_{16,m})^{z_1}(P_{36,m})^{z_3}\,, \quad (A.7)
$$

where

$$
\begin{aligned}
f^{(1)}(z_1,z_2,z_3) \;=\;& \Gamma(-z_1)\Gamma(-z_2)\Gamma(-z_3)\Gamma(1+z_1+z_3)\Gamma(1+z_2) \\
& \times \frac{\Gamma(-z_1-z_3)\Gamma(1+z_2+z_1)\Gamma(1+z_2+z_3)}{\Gamma(2(1+z_2))}\,. \quad (A.8)
\end{aligned}
$$

Plugging (A.7) into (A.3), we obtain

$$
I_{3a} = s^3\,t \int \frac{dz_{1,2,3}}{(2\pi i)^3}\, f^{(1)}(z_1,z_2,z_3)\, s^{z_2}(m^2)^{-1-z_2} \int \frac{d^4x_7}{i\pi^2}\, I_{3a}^{(2)}\,\big(P_{37,m}\,P_{17,m}\,P_{47,m}\big)^{-1}\,, \quad (A.9)
$$

where $I_{3a}^{(2)}$ is the integral over x_6:

$$
\begin{aligned}
I_{3a}^{(2)} \;=\;& \int \frac{d^4x_6}{i\pi^2}\,(P_{26,m})^{-1-z_1-z_3}(P_{16,m})^{-1+z_1}(P_{36,m})^{-1+z_3}(P_{67})^{-1} \\
\;=\;& \int_0^\infty \frac{d\alpha_i\,\delta(\sum\alpha_i-1)\,\alpha_1^{-z_1}\,\alpha_3^{-z_3}\,\alpha_2^{z_1+z_3}}{[\alpha_1\alpha_3 s+\alpha_7\,(\alpha_1 P_{17,m}+\alpha_2 P_{27,m}+\alpha_3 P_{37,m})+(\alpha_1+\alpha_2+\alpha_3)^2 m^2]^2} \\
& \times \frac{1}{\Gamma(1-z_1)\Gamma(1-z_3)\Gamma(1+z_1+z_3)} \quad (A.10)
\end{aligned}
$$

This is a generalization of the integral considered before with more general powers of the propagators. The calculation is completely analogous, and we obtain

$$
I_{3a}^{(2)} = \int \frac{dy_{1,2,3}}{(2\pi i)^3}\, f^{(2)}(z_{1,2,3};y_{1,2,3})\, s^{y_2}\,(m^2)^{-1-y_2}\,(P_{17,m})^{y_1}\,(P_{37,m})^{y_3}\,(P_{27,m})^{-1-y_1-y_3}\,, \quad (A.11)
$$

with

$$
\begin{aligned}
f^{(2)}(z_{1,2,3};y_{1,2,3}) \;=\;& \frac{\Gamma(-y_1)\Gamma(-y_2)\Gamma(-y_3)\Gamma(1+y_1+y_3)\Gamma(1+y_2)}{\Gamma(1-z_1)\Gamma(1-z_3)\Gamma(1+z_1+z_3)} \\
& \times \frac{\Gamma(1-z_1+y_1+y_2)\Gamma(z_1+z_3-y_1-y_3)\Gamma(1-z_3+y_2+y_3)}{\Gamma(2(1+y_2))}\,. \quad (A.12)
\end{aligned}
$$

At this point we note that, for a ladder diagram with more rungs, the next subintegral would be of the same type as the preceding one (up to a change of labels of MB parameters), see figure 7. In the next section, we will use this iterative structure to write down a MB parametrization for the L-rung ladder with L arbitrary.

Coming back to the three-loop ladder, we are left with the final integration over x_7, namely

$$I_{3a} = s^3 t \int \frac{dz_{1,2,3}}{(2\pi i)^3} \frac{dy_{1,2,3}}{(2\pi i)^3} f^{(1)}(z_{1,2,3}) f^{(2)}(z_{1,2,3}; y_{1,2,3}) s^{z_2+y_2} (m^2)^{-2-z_2-y_2} I_{3a}^{(3)}, \quad (A.13)$$

where

$$I_{3a}^{(3)} = \int \frac{d^4 x_7}{i\pi^2} (P_{27,m})^{-1-y_1-y_3} (P_{17,m})^{-1+y_1} (P_{37,m})^{-1+y_3} (P_{47,m})^{-1}. \quad (A.14)$$

Introducing parameter integrals we have

$$I_{3a}^{(3)} = \frac{1}{\Gamma(1-y_1)\Gamma(1+y_1+y_3)\Gamma(1-y_3)} \int_0^\infty \frac{d\beta_i \, \delta(\sum \beta_i - 1) \, \beta_1^{-y_1} \beta_2^{y_1+y_3} \beta_3^{-y_3}}{[\beta_1\beta_3 s + \beta_2\beta_4 t + (\beta_1+\beta_2+\beta_3+\beta_4)^2 m^2]^2}. \quad (A.15)$$

Obviously, here it is convenient to choose $\sum = \sum_{i=1}^4$. Introducing two more MB parameters, we find

$$I_{3a}^{(3)} = \int \frac{dz_{4,5}}{(2\pi i)^2} f^{(3)}(y_{1,2,3}; z_{4,5}) s^{z_4} t^{z_5} (m^2)^{-2-z_4-z_5}, \quad (A.16)$$

where

$$\begin{aligned} f^{(3)}(y_{1,2,3}; z_{4,5}) &= \frac{\Gamma(-z_4)\Gamma(-z_5)\Gamma(2+z_4+z_5)}{\Gamma(1-y_1)\Gamma(1-y_3)\Gamma(1+y_1+y_3)} \\ &\times \frac{\Gamma(1+z_5)\Gamma(1+y_1+y_3+z_5)\Gamma(1-y_1+z_4)\Gamma(1-y_3+z_4)}{\Gamma(2(2+z_4+z_5))}. \end{aligned} \quad (A.17)$$

Putting everything together we arrive at the final result (relabelling $z_{4,5} \to z_{7,8}$ and $y_{1,2,3} \to z_{4,5,6}$)

$$I_{3a} = \int \frac{dz_{1,2,3,4,5,6,7,8}}{(2\pi i)^8} f^{(1)}(z_{1,2,3}) f^{(2)}(z_{1,2,3}; z_{4,5,6}) f^{(3)}(z_{4,5,6}; z_{7,8}) \left(\frac{m^2}{s}\right)^{-3-z_2-z_5-z_7} \left(\frac{m^2}{t}\right)^{-1-z_8}. \quad (A.18)$$

In eq. (A.18) the integration contours are chosen parallel to the imaginary axis, with the real parts of the integration variables defined such that all arguments of the Γ functions have positive real part. An allowed choice is

$$z_1 = -\frac{1}{2}, z_2 = -\frac{1}{4}, z_3 = -\frac{1}{4}, z_4 = -\frac{3}{4}, z_5 = -\frac{1}{16}, z_6 = -\frac{15}{32}, z_7 = -\frac{9}{32}, z_8 = -\frac{13}{32}. \quad (A.19)$$
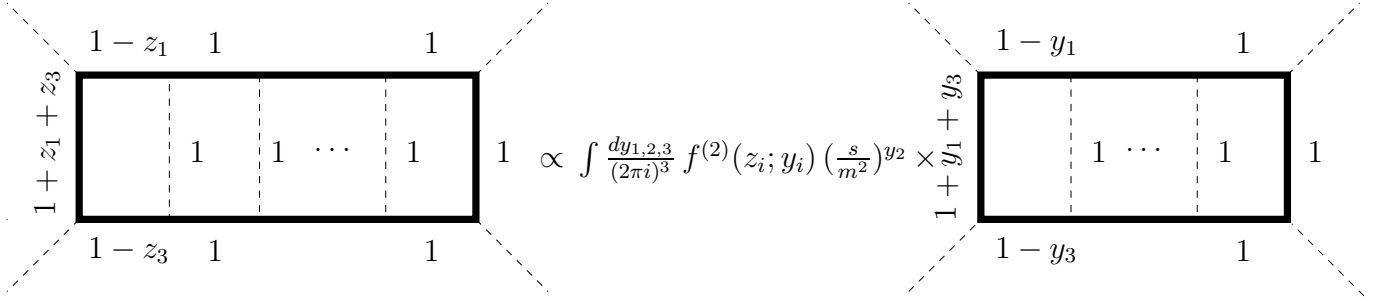
Figure 7: Diagrammatic representation of the iteration used to derive the L-loop MB representation for the ladder integral. Fat lines correspond to massive propagators, thin lines to massless ones. The numbers indicate the powers of the propagators. One can see that after removing a rung of the ladder (by introducing three Mellin-Barnes integrals) we obtain an integral of the same type, and the procedure can be iterated.

A.2   MB representation for the L-loop ladder diagram

As was noted in the previous section, one can straightforwardly write down an iterated MB formula for the L-loop ladder diagram. The decisive step is illustrated in figure 7. Let us define

$$I_{La} = s^L t \int \prod_{j=5}^{L+4} \left(\frac{d^4 x_j}{i\pi^2} \right) (P_{25,m} P_{15,m} P_{35,m})^{-1} \prod_{j=5}^{L+3} (P_{j,j+1} P_{1,j+1,m} P_{3,j+1,m})^{-1} (P_{4,L+4,m})^{-1} .$$

(A.20)

The MB formula we obtain is $(3L-1)$-fold and is given by (for $L > 1$)

$$
\begin{aligned}
I_{La} &= \int \prod_{j=1}^{L-1} \left(\frac{dz_{1,2,3}^{(j)}}{(2\pi i)^3} \right) \frac{dz_{4,5}}{(2\pi i)^2} \left(\frac{m^2}{s} \right)^{-L-\sum_{j=1}^{L-1} z_2^{(j)} - z_4} \left(\frac{m^2}{t} \right)^{-1-z_5} \\
&\times f^{(1)}(z_{1,2,3}^{(1)}) \prod_{j=1}^{L-2} f^{(2)}(z_{1,2,3}^{(j)}; z_{1,2,3}^{(j+1)}) f^{(3)}(z_{1,2,3}^{(L-1)}; z_{4,5}) .
\end{aligned}
$$

(A.21)

For completeness, we also give a formula for $L = 1$,

$$I_{1a} = I_1 = \int \frac{dz_{1,2}}{(2\pi i)^2} u^{-1-z_1} v^{-1-z_2} \frac{\Gamma(-z_1)\Gamma^2(1+z_1)\Gamma(-z_2)\Gamma^2(1+z_2)\Gamma(2+z_1+z_2)}{\Gamma(4+2z_1+2z_2)}$$

(A.22)

which is equivalent but more symmetric than the one given in ref. [25].

A.3   MB representation for the tennis court diagram

The procedure above can be repeated for the tennis court diagram (fig. 6b), which is given by

$$I_{3b} = s\, t^2 \int \frac{d^4 x_5 d^4 x_6 d^4 x_7}{(i\pi^2)^3} P_{17,m} (P_{25,m} P_{15,m} P_{57} P_{56} P_{16,m} P_{46,m} P_{67} P_{27,m} P_{37,m} P_{47,m})^{-1} .$$ (A.23)

A new feature of the tennis court is the presence of a numerator required by dual conformal symmetry. It is possible to treat this numerator as a propagator with negative power. However, this would require an analytical continuation, for example in the dimension of the integral, $D \to 4 - 2\epsilon$. Since our integral is finite in four dimensions, we find it preferable to perform the calculation in such a way that all steps can be done in four dimensions. This can be achieved by carrying out the two-loop ladder subintegral first (integrations over x_5 and x_6). The numerator will then combine in a natural way with a propagator obtained from this subintegral, allowing us to use a simple formula for the final integration over x_7.

As was explained above, we start by computing the subintegral $I_{3b}^{(1)}$ defined by

$$I_{3b}^{(1)} = \int \frac{d^4 x_5}{i\pi^2} \left(P_{25,m} P_{15,m} P_{57} P_{56} \right)^{-1} \tag{A.24}$$

where

$$I_{3b} = s\, t^2 \int \frac{d^4 x_6 d^4 x_7}{(i\pi^2)^2} P_{17,m} I_{3b}^{(1)} \left(P_{16,m} P_{46,m} P_{67} P_{27,m} P_{37,m} P_{47,m} \right)^{-1} . \tag{A.25}$$

It can be written as

$$I_{3b}^{(1)} = \int_0^\infty \frac{d\alpha_i\, \delta(\sum \alpha_1 + \alpha_2 - 1)}{[(P_{17,m}\alpha_1 + P_{27,m}\alpha_2)\alpha_7 + (P_{16,m}\alpha_1 + P_{26,m}\alpha_2)\alpha_6 + P_{67}\alpha_6\alpha_7 + m^2]^2} . \tag{A.26}$$

The integrals over α_6 and α_7 are done using eq. (A.42). Introducing two further MB integrals to factorize both b and c in eq. (A.42), we arrive at

$$I_{3b}^{(1)} = \int \frac{dz_{1,2,3}}{(2\pi i)^3} (m^2)^{-1-z_1} f_{3b}^{(1)} (P_{16,m})^{z_1 - z_3} (P_{27,m})^{z_1 - z_2} (P_{17,m})^{z_2} (P_{26,m})^{z_3} (P_{67})^{-1-z_1} \tag{A.27}$$

with

$$\begin{aligned}
f_{3b}^{(1)} &= \Gamma^2(1 + z_1)\Gamma(-z_2)\Gamma(-z_3)\Gamma(-z_1 + z_2)\Gamma(-z_1 + z_3) \\
&\quad \times \frac{\Gamma(1 + z_1 + z_2 - z_3)\Gamma(1 + z_1 - z_2 + z_3)}{\Gamma(2(1 + z_1))} .
\end{aligned} \tag{A.28}$$

Next, we want to carry out the x_6 integration in eq. (A.23). We define

$$I_{3b} \equiv s\, t^2 \int \frac{d^4 x_7}{i\pi^2} \frac{dz_{1,2,3}}{(2\pi i)^3} f_{3b}^{(1)} (m^2)^{-1-z_1} (P_{17,m})^{1+z_2} (P_{27,m})^{-1+z_1-z_2} (P_{37,m})^{-1} (P_{47,m})^{-1} I_{3b}^{(2)} . \tag{A.29}$$

Collecting all propagators involving x_6 in eqs. (A.23) and (A.27) we have

$$\begin{aligned}
I_{3b}^{(2)} &= \int \frac{d^4 x_6}{i\pi^2} (P_{67})^{-2-z_1} (P_{16,m})^{-1+z_1-z_3} (P_{26,m})^{z_3} (P_{46,m})^{-1} \tag{A.30} \\
&= \frac{1}{\Gamma(2+z_1)\Gamma(1-z_1+z_3)\Gamma(-z_3)} \int \frac{d\alpha_i\, \delta(\sum_{1,2,4}\alpha_i - 1)\, \alpha_1^{-z_1+z_3}\alpha_2^{-1-z_3}\alpha_7^{1+z_1}}{[t\alpha_2\alpha_4 + (P_{17,m}\alpha_1 + P_{27,m}\alpha_2 + P_{47,m}\alpha_4)\alpha_7 + m^2]^2} \\
&= \frac{\Gamma(-z_1)}{\Gamma(1-z_1+z_3)\Gamma(-z_3)} \int_0^1 d\alpha_i\, \delta(\sum_{1,2,4}\alpha_i - 1)\, \alpha_1^{-z_1+z_3}\alpha_2^{-1-z_3} \times \\
&\quad \times (t\alpha_2\alpha_4 + m^2)^{z_1} (P_{17,m}\alpha_1 + P_{27,m}\alpha_2 + P_{47,m}\alpha_4)^{-2-z_1} . \tag{A.31}
\end{aligned}$$

31

This is almost identical to an integral considered earlier for the ladder diagrams. Introducing MB parameters $z_{4,5,6}$ we find

$$I_{3b}^{(2)} = \int \frac{dz_{4,5,6}}{(2\pi i)^3} \, f_{3b}^{(2)} \, t^{z_4} \, (m^2)^{z_1 - z_4} \, (P_{17,m})^{z_5} \, (P_{27,m})^{z_6} \, (P_{47,m})^{-2 - z_1 - z_5 - z_6} \,, \tag{A.32}$$

with

$$\begin{aligned} f_{3b}^{(2)} &= \frac{\Gamma(-z_4)\Gamma(-z_1 + z_4)\Gamma(-z_5)\Gamma(-z_6)\Gamma(2 + z_1 + z_5 + z_6)}{\Gamma(2 + z_1)\Gamma(1 - z_1 + z_3)\Gamma(-z_3)\Gamma(2(-z_1 + z_4))} \times \\ &\quad \times \Gamma(1 - z_1 + z_3 + z_5)\Gamma(-z_3 + z_4 + z_6)\Gamma(-1 - z_1 + z_4 - z_5 - z_6) \,. \end{aligned} \tag{A.33}$$

Finally, we carry out the remaining integration over x_7,

$$I_{3b}^{(3)} \equiv \int \frac{d^4 x_7}{i\pi^2} \, (P_{17,m})^{1 + z_2 + z_5} \, (P_{27,m})^{-1 + z_1 - z_2 + z_6} \, (P_{37,m})^{-1} \, (P_{47,m})^{-3 - z_1 - z_5 - z_6} \,. \tag{A.34}$$

Up to a relabelling, this is the integral $I_{3a}^{(2)}$ of eqn (A.14). Hence we have

$$I_{3b}^{(3)} = \int \frac{dz_{7,8}}{(2\pi i)^2} \, f_{3b}^{(3)} \, s^{z_7} \, t^{z_8} \, (m^2)^{-2 - z_7 - z_8} \,, \tag{A.35}$$

with

$$\begin{aligned} f_{3b}^{(3)} &= \frac{\Gamma(-z_7)\Gamma(-z_8)\Gamma(2 + z_7 + z_8)}{\Gamma(1 - y_1)\Gamma(1 - y_3)\Gamma(1 + y_1 + y_3)\Gamma(2(2 + z_7 + z_8))} \times \\ &\quad \times \Gamma(1 + z_7)\Gamma(1 + y_1 + y_3 + z_7)\Gamma(1 - y_1 + z_8)\Gamma(1 - y_3 + z_8) \,. \end{aligned} \tag{A.36}$$

Here we have swapped s and t with respect to (A.16) and $y_1 \equiv -2 - z_1 - z_5 - z_6$ and $y_3 \equiv z_1 - z_2 + z_6$. Collecting all factors we obtain our final expression for the tennis court diagram

$$I_{3b} = \int \frac{dz_{1,2,3,4,5,6,7,8}}{(2\pi i)^8} \left(\frac{m^2}{s}\right)^{-1 - z_7} \left(\frac{m^2}{t}\right)^{-2 - z_4 - z_8} f_{3b}^{(1)} \, f_{3b}^{(2)} \, f_{3b}^{(3)} \,. \tag{A.37}$$

An allowed set of real parts for the integration variables is given by

$$z_1 = -\frac{11}{16}, \ z_2 = -\frac{1}{2}, \ z_3 = -\frac{7}{16}, \ z_4 = -\frac{1}{8}, \ z_5 = -\frac{9}{8}, \ z_6 = -\frac{3}{32}, \ z_7 = -\frac{13}{32}, \ z_8 = -\frac{1}{2}. \tag{A.38}$$

A.4   Auxiliary formulae

Here we collect some auxiliary formulae that were used in the derivations above. It is understood that the formulae below should be used within their region of validity, i.e. the real parts of the arguments of the Γ functions should be chosen positively.

$$(a+b)^{-\lambda} = \frac{1}{\Gamma(\lambda)} \int \frac{dz_2}{(2\pi i)} \Gamma(-z_2)\Gamma(\lambda+z_2) a^{z_2} b^{-\lambda-z_2} , \tag{A.39}$$

$$(a+b+c)^{-\lambda} = \frac{1}{\Gamma(\lambda)} \int \frac{dz_1 dz_3}{(2\pi i)^2} \Gamma(-z_1)\Gamma(-z_3)\Gamma(\lambda+z_1+z_3) \, a^{z_1} \, b^{z_3} \, c^{-\lambda-z_1-z_3} , \tag{A.40}$$

$$\int_0^\infty dx \, x^{z_1} (a+bx)^{z_2} = a^{1+z_1+z_2} b^{-1-z_1} \frac{\Gamma(1+z_1)\Gamma(-1-z_1-z_2)}{\Gamma(-z_2)} , \tag{A.41}$$

$$\int_0^\infty \frac{dx \, dy}{(a+bx+cy+dxy)^2} = (2\pi i)^{-1} \int dz (ad)^z (bc)^{-1-z} \Gamma^2(-z)\Gamma^2(1+z) , \tag{A.42}$$

$$\int_0^1 \prod_{i=1}^N d\alpha_i \alpha_i^{q_i-1} \delta(1 - \sum_{j=1}^N \alpha_j) = \frac{\Gamma(q_1)\dots\Gamma(q_N)}{\Gamma(q_1+\dots q_N)} . \tag{A.43}$$

B   Numerical evaluation using sector decomposition

Here we present an alternative, semi-numerical approach for evaluating the small m^2 expansion of integrals that is independent of the various MB representations derived above. We use the availability of powerful numerical algorithms for the calculation of the ϵ-expansion of parameter integrals [71, 74]. The expansion is done analytically, and only the coefficients of the poles are evaluated numerically. Therefore, this method avoids the problematic large logarithms that would appear in a direct numerical integration.

In order to use these algorithms, we need to reformulate our problem as a calculation of the ϵ-expansion of some parameter integral. Consider a generic four-dimensional L-loop diagram containing a propagators, where propagators with indices $i \in \mathcal{M}$ have mass m^2, and all other propagators are massless.[25] Then, the Feynman representation reads [73]

$$I = \Gamma(a-2L) \int d\alpha_i \, \delta(1 - \sum_i \alpha_i) \, U^{a-2L-2} \left[V(s,t) + U m^2 \sum_{i\in\mathcal{M}} \alpha_i \right]^{2L-a} \tag{B.1}$$

where U and $V(s,t)$ are polynomials in the α_i (see ref. [73] for more details).

We introduce one Mellin-Barnes parameter in order to separate off the mass dependence,

$$I = \int \frac{dz}{2\pi i} \Gamma(-z)\Gamma(a-2L+z) \, m^{2z} \, f(s,t,z) , \tag{B.2}$$

$$f(s,t,z) = \int d\alpha_i \, \delta(1 - \sum_i \alpha_i) \, (\sum_{i\in\mathcal{M}} \alpha_i)^z \, U^{a-2L-2+z} \, V(s,t)^{2L-a-z} , \tag{B.3}$$

with $2L-a < \text{Re}(z) < 0$. Note that $f(s,t,z)$ is very similar to a dimensionally-regulated massless Feynman diagram of the same topology.[26]

---

[25]Modifications are necessary for the case of integrals with numerator factors.

[26]A. Zhiboedov has independently written down a similar formula at one loop which exhibits the relation between massive and massless Feynman integrals (private communication).

Since we want to determine the behavior of I as $m^2 \to 0$ it is convenient to shift the integration contour in z to positive values of $\mathrm{Re}(z)$. In doing so, one picks up a residue from the pole at $z = 0$, and it is clear that the logarithms in m^2 will come from (minus) this residue.

$$I = -\mathrm{Residue}\left[\Gamma(-z)\Gamma(a - 2L + z)m^{2z} f(s,t,z)\right]\Bigg|_{z=0} + O(m^2). \tag{B.4}$$

The value of the latter can be obtained from the expansion of $\Gamma(-z)\Gamma(a - 2L + z)m^{2z}$ and $f(s,t,z)$ about $z = 0$. Therefore, in order to compute I up to and including order $\log^0(m^2)$, we need to evaluate $f(s,t,z)$ to order z^0. Note that we do not need terms that vanish as $z \to 0$. The coefficients of this expansion can be computed numerically using ref. [71].

We have tested this method for the two-loop ladder and found agreement with the result of ref. [25]. The method is also applicable to three-loop integrals but requires more computer time and memory.

C   Regge limit of the L-loop ladder diagram

In the two- and three-loop amplitudes considered in this paper, we see that the leading log behavior in the Regge (b) limit (see discussion in the introduction and in sec. 4) arises from the vertical ladder diagram. In this appendix, we will compute the first three leading terms in the Regge limit (b) of the ladder integral, employing an approach that was used in ref. [35].

The $s \gg t$ limit of the vertical ladder is equivalent to the $t \gg s$ limit of the horizontal ladder, and this is what we will now examine. The horizontal ladder diagram corresponds to the integral

$$I_{La} = s^L t \int \prod_{j=5}^{L+4} \left(\frac{d^4 x_j}{i\pi^2}\right) (P_{25,m}P_{15,m}P_{35,m})^{-1} \prod_{j=6}^{L+4}(P_{j-1,j}P_{1,j,m}P_{3,j,m})^{-1} (P_{4,L+4,m})^{-1} \tag{C.1}$$

where all the internal propagators are massless while the propagators on the periphery of the diagram have mass m. For each of the propagators, we use $(1/P) = i\int_0^\infty d\alpha \ \exp(-i\alpha P)$ to obtain

$$I_{La} = i^{3L+1} s^L t \int_0^\infty \prod_{k=0}^{L} d\alpha_k \prod_{l=1}^{L} d\beta_l \ d\gamma_l \int \prod_{j=5}^{L+4} \left(\frac{d^4 x_j}{i\pi^2}\right) \times \tag{C.2}$$

$$\times \exp\left[-i\alpha_0 P_{25,m} - i\sum_{k=1}^{L-1}\alpha_k P_{k+4,k+5} - i\alpha_L P_{4,L+4,m} - i\sum_{l=1}^{L}(\beta_l P_{1,l+4,m} + \gamma_l P_{3,l+4,m})\right].$$

Recalling that $P_{ij,m} = x_{ij}^2 + m^2$, we express the exponent as

$$-i\left(\mathbf{x^T} \cdot \mathbf{A} \cdot \mathbf{x} - 2\,\mathbf{B^T} \cdot \mathbf{x} + C + m^2\sigma\right) \tag{C.3}$$

where $\mathbf{x} = (x_5, \cdots, x_{L+4})$. We now integrate over $\mathbf{x}$ to obtain

$$I_{La} = i^{L+1} s^L t \int_0^\infty \prod_{k=0}^{L} d\alpha_k \prod_{l=1}^{L} d\beta_l \ d\gamma_l A^{-2} \exp\left[-i(C - \mathbf{B^T} \cdot \mathbf{A^{-1}} \cdot \mathbf{B} + m^2\sigma)\right]. \tag{C.4}$$

34

Setting $x_{12}^2 = x_{23}^2 = x_{34}^2 = x_{41}^2 = 0$, one has

$$C - \mathbf{B^T} \cdot \mathbf{A^{-1}} \cdot \mathbf{B} = s\frac{D_s}{A} + t\frac{D_t}{A}, \qquad \text{where } s = x_{13}^2 \quad \text{and } t = x_{24}^2. \tag{C.5}$$

Putting everything together, we have

$$I_{La} = i^{L+1} s^L t \int_0^\infty \prod_{k=0}^L d\alpha_k \prod_{l=1}^L d\beta_l \, d\gamma_l A^{-2} \exp\left[-it\frac{D_t}{A} - iJ\right], \qquad J = s\frac{D_s}{A} + m^2\sigma \tag{C.6}$$

where A, D_s, D_t, and σ are polynomials of degree L, $L+1$, $L+1$, and 1 in the α, β and γ's. These polynomials may be constructed using graphical rules [35, 73].

To explore the $t \gg s$ limit of the horizontal ladder diagram, it is useful to perform the Mellin transform [35]

$$M(\epsilon) = \int_0^\infty \frac{d\tau}{\tau^\epsilon} I_{La} \tag{C.7}$$

with respect to $\tau = t/m^2$. This gives

$$M(\epsilon) = \tau (is)^L (im^2)^\epsilon \Gamma(1-\epsilon) F(\epsilon) \tag{C.8}$$

where

$$F(\epsilon) = \int_0^\infty \prod_{k=0}^L d\alpha_k \prod_{l=1}^L d\beta_l \, d\gamma_l D_t^{\epsilon-1} A^{-1-\epsilon} \, \mathrm{e}^{-iJ}. \tag{C.9}$$

The large τ behavior of I_{La} is determined by the behavior of $M(\epsilon)$ near $\epsilon = 0$. However, $F(\epsilon)$ diverges at $\epsilon = 0$, since $D_t = \prod_{k=0}^L \alpha_i$, so we need to do a Laurent expansion about $\epsilon = 0$. First we integrate by parts with respect to each of the α_i to obtain

$$F(\epsilon) = \frac{1}{\epsilon^{L+1}} \int_0^\infty \prod_{k=0}^L (-d\alpha_k) \prod_{l=1}^L d\beta_l \, d\gamma_l \left(\prod_{k=0}^L \alpha_k\right)^\epsilon \frac{\partial^{L+1}}{\partial\alpha_0 \cdots \partial\alpha_L}\left(\frac{\mathrm{e}^{-iJ}}{A^{1+\epsilon}}\right) \tag{C.10}$$

where we have taken $\epsilon > 0$ so that the surface terms at $\alpha_k = 0$ vanish. Then writing

$$\left(\prod_{k=0}^L \alpha_k\right)^\epsilon = 1 + \left[\sum_{i=0}^L \alpha_i^\epsilon - (L+1)\right] + \left[\sum_{i<j}^L (\alpha_i\alpha_j)^\epsilon - L\sum_{i=0}^L \alpha_i^\epsilon + \frac{1}{2}L(L+1)\right] + \mathcal{O}(\epsilon^3) \tag{C.11}$$

we obtain

$$F(\epsilon) = \frac{1}{\epsilon^{L+1}}\left\{K + \left[\sum_{i=0}^L K_i - (L+1)K\right] + \left[\sum_{i<j}^L K_{ij} - L\sum_{i=0}^L K_i + \frac{1}{2}L(L+1)K\right] + \mathcal{O}(\epsilon^3)\right\} \tag{C.12}$$
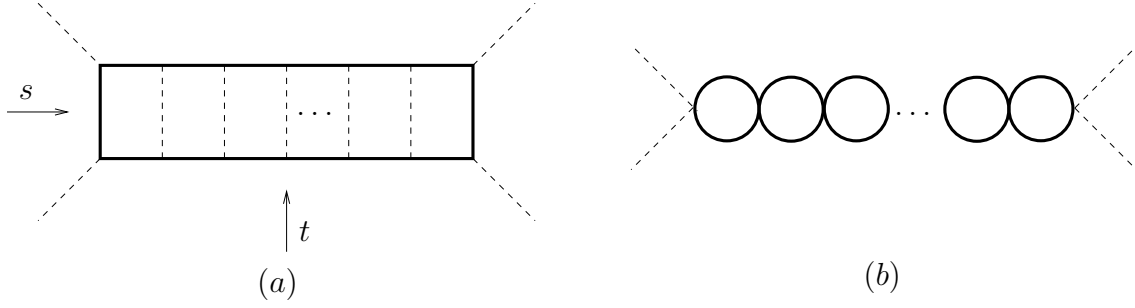
Figure 8: Factorization of the LL order contribution to the Regge limit $t \gg s$ of the horizontal L-loop ladder integral (a) into $(2 + 2\epsilon)$-dimensional bubble integrals (b).

where we have performed (most of) the integrations over α_i

$$
\begin{aligned}
K &= \int_0^\infty \prod_{l=1}^L d\beta_l \, d\gamma_l \left(\frac{\mathrm{e}^{-iJ}}{A^{1+\epsilon}} \right) \Bigg|_{\alpha_k=0} \\
K_i &= \int_0^\infty \prod_{l=1}^L d\beta_l \, d\gamma_l \, d\alpha_i \, \epsilon \, \alpha_i^{\epsilon-1} \left(\frac{\mathrm{e}^{-iJ}}{A^{1+\epsilon}} \right) \Bigg|_{\alpha_k=0, k\neq i} \\
K_{ij} &= \int_0^\infty \prod_{l=1}^L d\beta_l \, d\gamma_l \, d\alpha_i \, d\alpha_j \, \epsilon^2 \, \alpha_i^{\epsilon-1} \alpha_j^{\epsilon-1} \left(\frac{\mathrm{e}^{-iJ}}{A^{1+\epsilon}} \right) \Bigg|_{\alpha_k=0, k\neq i,j}.
\end{aligned}
\tag{C.13}
$$

The integrals in this equation may be interpreted as arising from (various deformations of) a horizontal L-loop ladder diagram in $d = 2 + 2\epsilon$ dimensions [73]. The rungs with $\alpha_k = 0$ are contracted to a point (and the corresponding propagator omitted), and the rungs with factors $\epsilon \alpha_i^{\epsilon-1}$ correspond to propagators raised to the power ϵ. Because most of the α_k are set to zero, the L-loop diagram separates into a product of smaller diagrams, and the integrals factorize. For example, when all $\alpha_k = 0$, we have

$$
A = \prod_{l=1}^L (\beta_l + \gamma_l), \qquad \frac{D_s}{A} = \sum_{l=1}^L \frac{\beta_l \gamma_l}{\beta_l + \gamma_l}, \qquad \sigma = \sum_{l=1}^L (\beta_l + \gamma_l),
\tag{C.14}
$$

so K separates into a product of one-loop bubble diagrams (cf. fig. 8)

$$
K = \left[(is)^{\epsilon-1} B_1 \right]^L
\tag{C.15}
$$

where the one-loop bubble is defined as

$$
B_1 \equiv s^{1-\epsilon} \int \frac{d^{2+2\epsilon} x_5}{i\pi^{1+\epsilon}} \frac{1}{P_{15,m} P_{35,m}} = (is)^{1-\epsilon} \int_0^\infty \frac{d\beta d\gamma}{(\beta + \gamma)^{1+\epsilon}} \exp\left[-is \frac{\beta \gamma}{\beta + \gamma} - im^2(\beta + \gamma) \right].
\tag{C.16}
$$

If we are only interested in the leading log (LL) behavior as $t \gg s$, we may set $\epsilon \to 0$, so that only the first term in eq. (C.12) contributes, and B_1 becomes a two-dimensional diagram. This
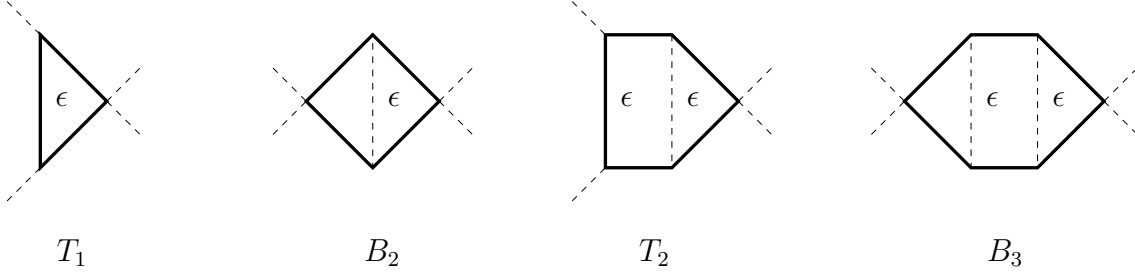
36

Figure 9: Integrals arising in the computation of the Regge limit of the horizontal L-loop ladder integral to NNLL order. The integration is in $2 + 2\epsilon$ dimensions.

was noted on p. 134 of ref. [35]. (See also chapter 8 of ref. [75].) Moreover, in this limit, the masses of the rungs of the original ladder diagram do not affect the result. Hence, in the LL limit, there is no distinction between the Higgs regulator considered here and the cutoff regulator considered in ref. [41].

Taking into account the factorization of the integrals in eq. (C.12), we obtain

$$
\begin{aligned}
F(\epsilon) &= \frac{(i^{\epsilon-1} B_1)^L}{\epsilon^{L+1}} \Big\{ 1 + \big[2t_1 + (L-1)b_2 - (L+1) \big] + \big[2t_2 + t_1{}^2 + 2(L-2)t_1 b_2 \\
&\quad + (L-2)b_3 + \frac{1}{2}(L-2)(L-3)b_2^2 - 2Lt_1 - L(L-1)b_2 + \frac{1}{2}L(L+1) \big] \Big\} \quad \text{(C.17)}
\end{aligned}
$$

with

$$
\begin{aligned}
t_1 &= \left(\frac{\Gamma(1+\epsilon)}{(is)^\epsilon} \right) \frac{T_1}{B_1}, & b_2 &= \left(\frac{\Gamma(1+\epsilon)}{(is)^\epsilon} \right) \frac{B_2}{B_1^2} \\
t_2 &= \left(\frac{\Gamma(1+\epsilon)}{(is)^\epsilon} \right)^2 \frac{T_2}{B_1^2}, & b_3 &= \left(\frac{\Gamma(1+\epsilon)}{(is)^\epsilon} \right)^2 \frac{B_3}{B_1^3}
\end{aligned} \quad \text{(C.18)}
$$

where T_1, B_2, T_2, and B_3 are the $(2 + 2\epsilon)$-dimensional diagrams shown in fig. 9, and defined by

$$
\begin{aligned}
T_1 &\equiv s \int \frac{d^{2+2\epsilon}x_5}{i\pi^{1+\epsilon}} \frac{1}{P_{15,m} P_{35,m} (P_{25,m})^\epsilon} \\
B_2 &\equiv s^{2-\epsilon} \int \frac{d^{2+2\epsilon}x_5}{i\pi^{1+\epsilon}} \int \frac{d^{2+2\epsilon}x_6}{i\pi^{1+\epsilon}} \frac{1}{P_{15,m} P_{16,m} P_{35,m} P_{36,m} (P_{56})^\epsilon} \\
T_2 &\equiv s^2 \int \frac{d^{2+2\epsilon}x_5}{i\pi^{1+\epsilon}} \int \frac{d^{2+2\epsilon}x_6}{i\pi^{1+\epsilon}} \frac{1}{P_{15,m} P_{16,m} P_{35,m} P_{36,m} (P_{25,m} P_{56})^\epsilon} \\
B_3 &\equiv s^{3-\epsilon} \int \frac{d^{2+2\epsilon}x_5}{i\pi^{1+\epsilon}} \int \frac{d^{2+2\epsilon}x_6}{i\pi^{1+\epsilon}} \int \frac{d^{2+2\epsilon}x_7}{i\pi^{1+\epsilon}} \frac{1}{P_{15,m} P_{16,m} P_{17,m} P_{35,m} P_{36,m} P_{37,m} (P_{56} P_{67})^\epsilon} \, .
\end{aligned} \quad \text{(C.19)}
$$

These integrals can be evaluated using MB techniques.

First consider the more general integral

$$
\int \frac{d^d x_5}{i\pi^{d/2}} (P_{13})^{a - \frac{d}{2}} (P_{15,m})^{-a_1} (P_{25,m})^{-a_2} (P_{35,m})^{-a_3} = \int \frac{dz}{(2\pi i)} g_1(a_1, a_2, a_3; d; z) u^{-z - a + \frac{d}{2}} \quad \text{(C.20)}
$$

37

where $a = a_1 + a_2 + a_3$ and $u = m^2/s$ and

$$g_1(a_1, a_2, a_3; d; z) = \frac{\Gamma(-z)\Gamma(a - \frac{d}{2} + z)\Gamma(a_1 + z)\Gamma(a_3 + z)}{\Gamma(a_1)\Gamma(a_3)\Gamma(2z + a)} . \qquad \text{(C.21)}$$

We will also need

$$\int \frac{d^d x_5}{i\pi^{d/2}} (P_{13})^{a-\frac{d}{2}} (P_{15,m})^{-a_1} (P_{35,m})^{-a_3} (P_{65})^{-a_6}$$

$$= \int \frac{dz_1\, dz_2\, dz_3}{(2\pi i)^3} \, g_2(a_1, a_3, a_6; d; z_i) \, (P_{13})^{-z_1-z_3} (P_{16,m})^{z_1} (P_{36,m})^{z_3} \, u^{-z-a+\frac{d}{2}} \quad \text{(C.22)}$$

where $a = a_1 + a_3 + a_6$ and $z = z_1 + z_2 + z_3$ and

$$g_2(a_1, a_3, a_6; d; z_i) \;=\; \frac{\Gamma(-z_1)\Gamma(-z_2)\Gamma(-z_3)}{\Gamma(a_1)\Gamma(a_3)\Gamma(a_6)}\Gamma\left(a - \frac{d}{2} + z\right) \times \qquad \text{(C.23)}$$

$$\times \;\; \frac{\Gamma(a_1 + z_1 + z_2)\Gamma(a_3 + z_2 + z_3)\Gamma(a_6 + z_1 + z_3)\Gamma(d - a - a_6 - z_1 - z_3)}{\Gamma(a_1 + a_3 + z + z_2)\Gamma(d - a)} .$$

Then we may write

$$B_1 \;=\; \int \frac{dz}{(2\pi i)} \, g_1(1, 0, 1; 2 + 2\epsilon; z) \, u^{-1+\epsilon-z} ,$$

$$T_1 \;=\; \int \frac{dz}{(2\pi i)} \, g_1(1, \epsilon, 1; 2 + 2\epsilon; z) \, u^{-1-z} ,$$

$$B_2 \;=\; \int \frac{d^4 z}{(2\pi i)^4} \, g_2(1, 1, \epsilon; 2 + 2\epsilon; z_{1,2,3}) \, g_1(1 - z_1, 0, 1 - z_3; 2 + 2\epsilon; z_4) \, u^{-2+\epsilon-z_2-z_4} ,$$

$$T_2 \;=\; \int \frac{d^4 z}{(2\pi i)^4} \, g_2(1, 1, \epsilon; 2 + 2\epsilon; z_{1,2,3}) \, g_1(1 - z_1, \epsilon, 1 - z_3; 2 + 2\epsilon; z_4) \, u^{-2-z_2-z_4} ,$$

$$B_3 \;=\; \int \frac{d^7 z}{(2\pi i)^7} \, g_2(1, 1, \epsilon; 2 + 2\epsilon; z_{1,2,3}) \, g_2(1 - z_1, 1 - z_3, \epsilon; 2 + 2\epsilon; z_{4,5,6})$$

$$\times \;\; g_1(1 - z_4, 0, 1 - z_6; 2 + 2\epsilon; z_7) u^{-3+\epsilon-z_2-z_5-z_7} . \qquad \text{(C.24)}$$

Note that some of the MB representations above require an analytic continuation to $\epsilon \approx 0$. In some cases this may reduce the number of MB integrals. Expanding around $\epsilon = 0$ (after having

taken the analytic continuation where required) and then expanding in small u we find[27]

$$
\begin{aligned}
e^{-\epsilon\gamma_E} B_1 &= -2\log u + \epsilon\left[-\log^2 u - \frac{1}{3}\pi^2\right] + \epsilon^2\left[-\frac{1}{3}\log^3 u - \frac{1}{6}\pi^2\log u + 4\zeta_3\right] + \dots \\
e^{-\epsilon\gamma_E} T_1 &= -2\log u + \epsilon\left[\frac{1}{2}\log^2 u - \frac{2}{3}\pi^2\right] + \epsilon^2\left[\frac{1}{2}\pi^2\log u + 8\zeta_3\right] + \dots \\
e^{-2\epsilon\gamma_E} B_2 &= 4\log^2 u + \epsilon\left[\frac{10}{3}\log^3 u + \frac{4}{3}\pi^2\log u + 4\zeta_3\right] \\
&\quad + \epsilon^2\left[\frac{5}{3}\log^4 u + \pi^2\log^2 u + 4\zeta_3\log u + \frac{2}{15}\pi^4\right] + \dots \\
e^{-2\epsilon\gamma_E} T_2 &= 4\log^2 u + \epsilon\left[\frac{1}{3}\log^3 u + 2\pi^2\log u + 4\zeta_3\right] + \epsilon^2\left[\frac{5}{24}\log^4 u + \frac{31}{90}\pi^4\right] + \dots \\
e^{-3\epsilon\gamma_E} B_3 &= -8\log^3 u + \epsilon\left[-\frac{28}{3}\log^4 u - 4\pi^2\log^2 u - 16\zeta_3\log u\right] + \\
&\quad + \epsilon^2\left[-\frac{94}{15}\log^5 u - \frac{38}{9}\pi^2\log^3 u - 20\zeta_3\log^2 u - \frac{34}{45}\pi^4\log u - 44.705\right] + \dots
\end{aligned}
$$

$$(\text{C.25})$$

Combining eqs. (C.8), (C.17), (C.18), and (C.25), we obtain

$$
\begin{aligned}
M(\epsilon) &= \tau\frac{(-2)^L}{\epsilon^{L+1}}\Bigg\{1 + \epsilon\left[\frac{L-1}{3}\log^{L+1} u + \frac{L+2}{6}\pi^2\log^{L-1} u + (L-1)\zeta_3\log^{L-2} u\right] \\
&\quad + \epsilon^2\left[\frac{10L^2 - 14L + 3}{180}\log^{L+2} u + \frac{(L+1)^2}{18}\pi^2\log^L u + \frac{L(L-2)}{3}\zeta_3\log^{L-1} u \right.\\
&\quad + \frac{(L+3)(5L+2)}{360}\pi^4\log^{L-2} u + \frac{L-2}{6}(L+1.826)\pi^2\zeta_3\log^{L-3} u \\
&\quad \left.+ \frac{(L-2)(L-3)}{2}\zeta_3^2\log^{L-4} u\right] + \mathcal{O}(\epsilon^3)\Bigg\}.
\end{aligned}
$$

$$(\text{C.26})$$

To take the inverse Mellin transform, we use [35]

$$
M(\epsilon) = \frac{1}{\epsilon^{n+1}} \implies I = \frac{1}{n!}\frac{\log^n \tau}{\tau}
$$

$$(\text{C.27})$$

---

[27]The coefficients of the π^4 terms were obtained numerically, and replaced by their probable rational equivalents.

so that the first three leading log terms of the ladder diagram are given by

$$
\lim_{u,v\ll 1}\lim_{v\ll u} I_{La}(u,v) = \frac{2^L}{L!}\log^L v\log^L u
$$

$$
- \frac{2^L}{(L-1)!}\log^{L-1} v\left[\frac{1}{3}(L-1)\log^{L+1} u + (L+2)\zeta_2\log^{L-1} u + (L-1)\zeta_3\log^{L-2} u\right]
$$

$$
+ \frac{2^L}{(L-2)!}\log^{L-2} v\left[\frac{10L^2-14L+3}{180}\log^{L+2} u + \frac{(L+1)^2}{18}\pi^2\log^L u\right.
$$

$$
+ \frac{L(L-2)}{3}\zeta_3\log^{L-1} u + \frac{(L+3)(5L+2)}{360}\pi^4\log^{L-2} u + \frac{L-2}{6}(L+1.826)\pi^2\zeta_3\log^{L-3} u
$$

$$
\left.+ \frac{(L-2)(L-3)}{2}\zeta_3^2\log^{L-4} u\right] + \mathcal{O}(\log^{L-3} v) \tag{C.28}
$$

where we recall that $v = m^2/t = 1/\tau$. This result is used in sec. 4.

References

[1] C. Anastasiou, Z. Bern, L. J. Dixon and D. A. Kosower, "Planar amplitudes in maximally supersymmetric Yang-Mills theory," Phys. Rev. Lett. **91** (2003) 251602 [arXiv:hep-th/0309040].

[2] Z. Bern, L. J. Dixon and V. A. Smirnov, "Iteration of planar amplitudes in maximally supersymmetric Yang-Mills theory at three loops and beyond," Phys. Rev. D **72** (2005) 085001 [arXiv:hep-th/0505205].

[3] J. M. Drummond, J. Henn, G. P. Korchemsky and E. Sokatchev, "On planar gluon amplitudes/Wilson loops duality," Nucl. Phys. B **795** (2008) 52 [arXiv:0709.2368 [hep-th]].

[4] L. F. Alday and J. Maldacena, "Comments on gluon scattering amplitudes via AdS/CFT," JHEP **0711**, 068 (2007) [arXiv:0710.1060 [hep-th]].

[5] Z. Bern, L. J. Dixon, D. A. Kosower, R. Roiban, M. Spradlin, C. Vergu and A. Volovich, "The Two-Loop Six-Gluon MHV Amplitude in Maximally Supersymmetric Yang-Mills Theory," Phys. Rev. D **78** (2008) 045007 [arXiv:0803.1465 [hep-th]].

[6] J. M. Drummond, J. Henn, G. P. Korchemsky and E. Sokatchev, "Hexagon Wilson loop = six-gluon MHV amplitude," Nucl. Phys. B **815**, 142 (2009) [arXiv:0803.1466 [hep-th]].

[7] V. Del Duca, C. Duhr and V. A. Smirnov, "An Analytic Result for the Two-Loop Hexagon Wilson Loop in $\mathcal{N} = 4$ SYM," arXiv:0911.5332 [hep-ph].

[8] J. M. Drummond, J. Henn, V. A. Smirnov and E. Sokatchev, "Magic identities for conformal four-point integrals," JHEP **0701** (2007) 064 [arXiv:hep-th/0607160].

[9] L. F. Alday and J. M. Maldacena, "Gluon scattering amplitudes at strong coupling," JHEP **0706** (2007) 064 [arXiv:0705.0303 [hep-th]].

[10] J. M. Drummond, G. P. Korchemsky and E. Sokatchev, "Conformal properties of four-gluon planar amplitudes and Wilson loops," Nucl. Phys. B **795**, 385 (2008) [arXiv:0707.0243 [hep-th]].

[11] A. Brandhuber, P. Heslop and G. Travaglini, "MHV Amplitudes in $\mathcal{N} = 4$ Super Yang-Mills and Wilson Loops," Nucl. Phys. B **794** (2008) 231 [arXiv:0707.1153 [hep-th]].

[12] L. F. Alday and R. Roiban, "Scattering Amplitudes, Wilson Loops and the String/Gauge Theory Correspondence," Phys. Rept. **468**, 153 (2008) [arXiv:0807.1889 [hep-th]].

[13] J. M. Henn, "Duality between Wilson loops and gluon amplitudes," Fortsch. Phys. **57**, 729 (2009) [arXiv:0903.0522 [hep-th]].

[14] J. M. Drummond, J. Henn, G. P. Korchemsky and E. Sokatchev, "Conformal Ward identities for Wilson loops and a test of the duality with gluon amplitudes," Nucl. Phys. B **826** (2010) 337 [arXiv:0712.1223 [hep-th]].

[15] J. M. Drummond, J. Henn, G. P. Korchemsky and E. Sokatchev, "Dual superconformal symmetry of scattering amplitudes in $\mathcal{N} = 4$ super-Yang-Mills theory," Nucl. Phys. B **828**, 317 (2010) [arXiv:0807.1095 [hep-th]].

[16] A. Brandhuber, P. Heslop and G. Travaglini, "A note on dual superconformal symmetry of the $\mathcal{N} = 4$ super Yang-Mills S-matrix," Phys. Rev. D **78** (2008) 125005 [arXiv:0807.4097 [hep-th]].

[17] J. M. Drummond and J. M. Henn, "All tree-level amplitudes in $\mathcal{N} = 4$ SYM," JHEP **0904** (2009) 018 [arXiv:0808.2475 [hep-th]].

[18] N. Berkovits and J. Maldacena, "Fermionic T-Duality, Dual Superconformal Symmetry, and the Amplitude/Wilson Loop Connection," JHEP **0809** (2008) 062 [arXiv:0807.3196 [hep-th]].

[19] N. Beisert, R. Ricci, A. A. Tseytlin and M. Wolf, "Dual Superconformal Symmetry from $AdS_5 \times S^5$ Superstring Integrability," Phys. Rev. D **78** (2008) 126004 [arXiv:0807.3228 [hep-th]].

[20] N. Beisert, "T-Duality, Dual Conformal Symmetry and Integrability for Strings on AdS_5xS^5," Fortsch. Phys. **57** (2009) 329 [arXiv:0903.0609 [hep-th]].

[21] J. M. Drummond, J. M. Henn and J. Plefka, "Yangian symmetry of scattering amplitudes in $\mathcal{N} = 4$ super Yang-Mills theory," JHEP **0905** (2009) 046 [arXiv:0902.2987 [hep-th]].

[22] G. P. Korchemsky and E. Sokatchev, "Symmetries and analytic properties of scattering amplitudes in $\mathcal{N} = 4$ SYM theory," arXiv:0906.1737 [hep-th].

[23] T. Bargheer, N. Beisert, W. Galleas, F. Loebbert and T. McLoughlin, "Exacting $\mathcal{N} = 4$ Superconformal Symmetry," JHEP **0911** (2009) 056 [arXiv:0905.3738 [hep-th]].

[24] A. Sever and P. Vieira, "Symmetries of the $\mathcal{N} = 4$ SYM S-matrix," arXiv:0908.2437 [hep-th].

[25] L. F. Alday, J. M. Henn, J. Plefka and T. Schuster, "Scattering into the fifth dimension of $\mathcal{N} = 4$ super Yang-Mills," arXiv:0908.0684 [hep-th].

[26] H. Kawai and T. Suyama, "Some Implications of Perturbative Approach to AdS/CFT Correspondence," Nucl. Phys. B **794** (2008) 1 [arXiv:0708.2463 [hep-th]].

[27] R. M. Schabinger, "Scattering on the Moduli Space of $\mathcal{N} = 4$ Super Yang-Mills," arXiv:0801.1542 [hep-th].

[28] J. McGreevy and A. Sever, "Planar scattering amplitudes from Wilson loops," JHEP **0808** (2008) 078 [arXiv:0806.0668 [hep-th]].

[29] A. Mitov and S. Moch, "The singular behavior of massive QCD amplitudes," JHEP **0705** (2007) 001 [arXiv:hep-ph/0612149].

[30] S. G. Naculich and H. J. Schnitzer, "Regge behavior of gluon scattering amplitudes in $\mathcal{N} = 4$ SYM theory," Nucl. Phys. B **794**, 189 (2008) [arXiv:0708.3069 [hep-th]].

[31] V. Del Duca and E. W. N. Glover, "Testing high-energy factorization beyond the next-to-leading-logarithmic accuracy," JHEP **0805**, 056 (2008) [arXiv:0802.4445 [hep-th]].

[32] S. G. Naculich and H. J. Schnitzer, "IR divergences and Regge limits of subleading-color contributions to the four-gluon amplitude in $\mathcal{N} = 4$ SYM Theory," JHEP **0910**, 048 (2009) [arXiv:0907.1895 [hep-th]].

[33] V. Del Duca, C. Duhr and E. W. N. Glover, "Iterated amplitudes in the high-energy limit," JHEP **0812**, 097 (2008) [arXiv:0809.1822**v4** [hep-th]].

[34] V. Del Duca, C. Duhr and E. W. N. Glover, "Iterated amplitudes in the high-energy limit," [arXiv:0809.1822**v5** [hep-th]].

[35] R. J. Eden, P. V. Landshoff, D. I. Olive, and J. C. Polkinghorne, *The Analytic S-Matrix* (Cambridge University Press, Cambridge, 1966).

[36] R. C. Brower, H. Nastase, H. J. Schnitzer and C. I. Tan, "Implications of multi-Regge limits for the Bern-Dixon-Smirnov conjecture," Nucl. Phys. B **814**, 293 (2009) [arXiv:0801.3891 [hep-th]].

[37] J. Bartels, L. N. Lipatov and A. Sabio Vera, "BFKL Pomeron, Reggeized gluons and Bern-Dixon-Smirnov amplitudes," Phys. Rev. D **80**, 045002 (2009) [arXiv:0802.2065 [hep-th]].

[38] J. Bartels, L. N. Lipatov and A. Sabio Vera, "$\mathcal{N} = 4$ supersymmetric Yang Mills scattering amplitudes at high energies: the Regge cut contribution," arXiv:0807.0894 [hep-th].

[39] R. C. Brower, H. Nastase, H. J. Schnitzer and C. I. Tan, "Analyticity for Multi-Regge Limits of the Bern-Dixon-Smirnov Amplitudes," Nucl. Phys. B **822**, 301 (2009) [arXiv:0809.1632 [hep-th]].

[40] R. M. Schabinger, "The Imaginary Part of the $\mathcal{N} = 4$ Super-Yang-Mills Two-Loop Six-Point MHV Amplitude in Multi-Regge Kinematics," JHEP **0911** (2009) 108 [arXiv:0910.3933 [hep-th]].

[41] H. J. Schnitzer, "Reggeization of $\mathcal{N} = 8$ Supergravity and $\mathcal{N} = 4$ Yang-Mills Theory II," arXiv:0706.0917 [hep-th].

[42] M. L. Mangano, S. J. Parke and Z. Xu, "Duality and Multi-Gluon Scattering," Nucl. Phys. B **298**, 653 (1988).

[43] F. A. Berends and W. Giele, "The Six Gluon Process As An Example Of Weyl-Van Der Waerden Spinor Calculus," Nucl. Phys. B **294**, 700 (1987).

[44] M. L. Mangano, "The Color Structure Of Gluon Emission," Nucl. Phys. B **309**, 461 (1988).

[45] D. J. Broadhurst, "Summation of an infinite series of ladder diagrams," Phys. Lett. B **307** (1993) 132.

[46] Z. Bern, M. Czakon, L. J. Dixon, D. A. Kosower and V. A. Smirnov, "The Four-Loop Planar Amplitude and Cusp Anomalous Dimension in Maximally Supersymmetric Yang-Mills Theory," Phys. Rev. D **75** (2007) 085010 [arXiv:hep-th/0610248].

[47] Z. Bern, J. J. M. Carrasco, H. Johansson and D. A. Kosower, "Maximally supersymmetric planar Yang-Mills amplitudes at five loops," Phys. Rev. D **76** (2007) 125020 [arXiv:0705.1864 [hep-th]].

[48] J. M. Drummond, J. Henn, G. P. Korchemsky and E. Sokatchev, "Generalized unitarity for $\mathcal{N} = 4$ super-amplitudes," arXiv:0808.0491 [hep-th].

[49] A. Brandhuber, P. Heslop and G. Travaglini, "One-Loop Amplitudes in $\mathcal{N} = 4$ Super Yang-Mills and Anomalous Dual Conformal Symmetry," JHEP **0908** (2009) 095 [arXiv:0905.4377 [hep-th]].

[50] H. Elvang, D. Z. Freedman and M. Kiermaier, "Dual conformal symmetry of 1-loop NMHV amplitudes in $\mathcal{N} = 4$ SYM theory," arXiv:0905.4379 [hep-th].

[51] A. Brandhuber, P. Heslop and G. Travaglini, "Proof of the Dual Conformal Anomaly of One-Loop Amplitudes in $\mathcal{N} = 4$ SYM," JHEP **0910** (2009) 063 [arXiv:0906.3552 [hep-th]].

[52] I. A. Korchemskaya and G. P. Korchemsky, "On lightlike Wilson loops," Phys. Lett. B **287** (1992) 169.

[53] V. A. Smirnov, "Analytical result for dimensionally regularized massless on-shell double box," Phys. Lett. B **460**, 397 (1999) [arXiv:hep-ph/9905323].

[54] D. Nguyen, M. Spradlin and A. Volovich, "New Dual Conformally Invariant Off-Shell Integrals," Phys. Rev. D **77** (2008) 025018 [arXiv:0709.4665 [hep-th]].

[55] Z. Bern, L. J. Dixon, D. C. Dunbar and D. A. Kosower, "One-Loop n-Point Gauge Theory Amplitudes, Unitarity and Collinear Limits," Nucl. Phys. B **425**, 217 (1994) [arXiv:hep-ph/9403226].

[56] Z. Bern, L. J. Dixon, D. C. Dunbar and D. A. Kosower, "Fusing gauge theory tree amplitudes into loop amplitudes," Nucl. Phys. B **435**, 59 (1995) [arXiv:hep-ph/9409265].

[57] E. I. Buchbinder and F. Cachazo, "Two-loop amplitudes of gluons and octa-cuts in $\mathcal{N} = 4$ super Yang-Mills," JHEP **0511** (2005) 036 [arXiv:hep-th/0506126].

[58] F. Cachazo and D. Skinner, "On the structure of scattering amplitudes in $\mathcal{N} = 4$ super Yang-Mills and $\mathcal{N} = 8$ supergravity," arXiv:0801.4574 [hep-th].

[59] S. Mandelstam, "Non-Regge Terms in the Vector-Spinor Theory," Phys. Rev. **137** (1965) B949.

[60] M. T. Grisaru, H. J. Schnitzer and H. S. Tsao, "Reggeization of yang-mills gauge mesons in theories with a spontaneously broken symmetry," Phys. Rev. Lett. **30** (1973) 811;

[61] M. T. Grisaru, H. J. Schnitzer and H. S. Tsao, "Reggeization of elementary particles in renormalizable gauge theories - vectors and spinors," Phys. Rev. D **8**, 4498 (1973).

[62] M. T. Grisaru and H. J. Schnitzer, "Reggeization Of Gauge Vector Mesons And Unified Theories," Phys. Rev. D **20**, 784 (1979).

[63] M. T. Grisaru and H. J. Schnitzer, "Bound States In $\mathcal{N} = 8$ Supergravity And $\mathcal{N} = 4$ Supersymmetric Yang-Mills Theories," Nucl. Phys. B **204** (1982) 267.

[64] J. Gluza, K. Kajda and T. Riemann, "AMBRE - a Mathematica package for the construction of Mellin-Barnes representations for Feynman integrals," Comput. Phys. Commun. **177** (2007) 879 [arXiv:0704.2423 [hep-ph]].

[65] A. M. Polyakov, "Gauge Fields As Rings Of Glue," Nucl. Phys. B **164** (1980) 171.

[66] G. P. Korchemsky and A. V. Radyushkin, "Loop Space Formalism And Renormalization Group For The Infrared Asymptotics Of QCD," Phys. Lett. B **171** (1986) 459.

[67] S. V. Ivanov, G. P. Korchemsky and A. V. Radyushkin, "Infrared Asymptotics Of Perturbative QCD: Contour Gauges," Yad. Fiz. **44** (1986) 230 [Sov. J. Nucl. Phys. **44** (1986) 145].

[68] G. P. Korchemsky and A. V. Radyushkin, "Renormalization of the Wilson Loops Beyond the Leading Order," Nucl. Phys. B **283** (1987) 342.

[69] G. P. Korchemsky and A. V. Radyushkin, "Infrared factorization, Wilson lines and the heavy quark limit," Phys. Lett. B **279** (1992) 359 [arXiv:hep-ph/9203222].

[70] M. Czakon, "Automatized analytic continuation of Mellin-Barnes integrals," Comput. Phys. Commun. **175** (2006) 559 [arXiv:hep-ph/0511200].

[71] C. Bogner and S. Weinzierl, "Resolution of singularities for multi-loop integrals," Comput. Phys. Commun. **178** (2008) 596 [arXiv:0709.4092 [hep-ph]].

[72] N. I. Usyukina and A. I. Davydychev, "An Approach to the evaluation of three and four point ladder diagrams," Phys. Lett. B **298**, 363 (1993).

[73] V. A. Smirnov, *Feynman integral calculus* (Springer-Verlag, Berlin, 2006).

[74] T. Binoth and G. Heinrich, "An automatized algorithm to compute infrared divergent multi-loop integrals," Nucl. Phys. B **585** (2000) 741 [arXiv:hep-ph/0004013].

[75] V. N. Gribov, *The Theory of Complex Angular Momenta* (Cambridge University Press, Cambridge, 2003).